PHILOSOPHICAL TRANSACTIONS OF THE ROYAL SOCIETY A MATHEMATICAL, PHYSICAL & ENGINEERING SCIENCES

A Unified Analysis of Tides and Surges Round North and East Britain

D. E. Cartwright

Phil. Trans. R. Soc. Lond. A 1968 **263**, 1-55
doi: 10.1098/rsta.1968.0005

A UNIFIED ANALYSIS OF TIDES AND SURGES ROUND NORTH AND EAST BRITAIN

By D. E. CARTWRIGHT

National Institute of Oceanography, Wormley, Godalming, Surrey

(*Communicated by G. E. R. Deacon, F.R.S.—Received* 17 *July* 1967)

CONTENTS

Tide gauge records from six ports round north and east Britain are analysed in terms of the response of sea level to gravitational and radiational tide potentials, and to a six-component function which describes the major features of the weather over the relevant sea area. Tidal interaction effects due to shallow water are allowed for up to third order. The linear tidal admittances in species 1, 2 and 3 are found to be smooth and consistent from one port to another. The radiational components are found to have amplitudes around 18% of the 12 h tide due to gravity at all ports, with consistent phase leads on the gravitational tide. The second-order interactions producing tides of species 4 are found to have strong dependence on frequency, and are surprisingly noisy at Southend. The third-order tides at species 6 have neither of these properties, and their amplitudes are shown to vary approximately with the cube of the main tidal amplitude. This last fact is reconciled with a quadratic frictional law. On the whole, the response analysis of the tides is found to be more accurate than a harmonic analysis which uses a greater number of arbitrary constants, with an increasing improvement in predictable variance at the shallower ports.

At the two estuarine ports, effects coherent with interaction between tides and random variations in local sea level are found by a bispectral analysis. The interaction coefficients are reasonably consistent with those derived from the tides alone, and with computations by G. W. Lennon of wave propagation in the Thames Estuary. The interaction with local sea level is insufficient to account for the tidal modulations with frequencies less than 1 cycle/month. The spectra of these modulations at the M_2 frequency $\pm f$ are strongly coherent, and show similar proportions of phase- and amplitude-modulations at all stations. They may be due to oceanic, local, or instrumental effects. The seasonal effects at $f = \pm 1$ cycle/year stand out clearly, and point to a third distinct agent of tidal modulation.

The functions chosen to describe the weather are the first six coefficients of a special Taylor expansion of atmospheric pressure. As well as describing the field of normal stress, these functions implicitly embody a linearized wind stress through the pressure gradients. Inter-correlation between the six components are allowed for. They are all found to give significant contributions to sea level variance, and their responses extend to at least 24 h time delay.

Vol. 263. A. 1134. (Price £1. 9s.; U.S. $3.80) 1 [Published 4 April 1968

An array of three stations, Malin Head, Stornoway and Lerwick, is tested for detecting 'external surges' arriving as free waves at Aberdeen, but only Stornoway is found to be usable from the point of view of prediction. Self-prediction of consistent (low frequency and tidal) errors in the prediction of sea level by other variables is shown to be effective and useful.

Finally, the noise level in low frequency sea level is reduced by subtracting its purely weather-dependent part, to reveal significant values of the monthly and fortnightly tides. Their amplitudes are found to be surprisingly large (ratios of order 1) in relation to the zonal equilibrium tide.

1. Introduction

This paper differs from the many published studies of storm surges in the North Sea principally in that the surges are treated on an equal footing with the tides. Both are expressed as the response of the sea level to external forces which are more or less known. Munk & Cartwright (1966)—referred to hereafter as 'M.C.'—showed how the tide at any particular place could be analysed and predicted as a weakly nonlinear response to the gravitation and radiation potential of the Moon and Sun. The results were somewhat simpler and more accurate than predictions using the classical 'harmonic' method of tidal analysis. They were also more revealing physically, in that they separated the responses to different sorts of potential and their linear and nonlinear parts. In this paper, 'the response method' of M.C. is applied more widely, to the tide at a series of ports at roughly 200 miles intervals with large variations of shallow-water distortion. Also it is extended to evaluate the linear responses of the local sea level to various distinct characteristics of the weather disturbance over the whole sea area, and the nonlinear interactions between surge and tide.

There is of course an essential distinction. The tide at any place depends on forces acting over all the world's oceans, so that these forces (or their potentials) must be defined globally. Luckily, this can conveniently be done by a rapidly convergent expansion in spherical harmonics. The meteorological disturbance, on the other hand, is usually considered to be largely generated in local shelf seas, partly because the horizontal scale of weather variations in our latitudes is much smaller than that of the tide potential, and, more importantly, because the effects of tangential wind stress and of travelling depressions increases with decreasing depth of water. These forces can therefore be defined well enough by a spatial Taylor expansion valid over local waters. (I also allow for an 'external surge' due to weather forces outside the local area, to be discussed later.) Further, since the wind is itself closely related to the horizontal gradient of atmospheric pressure, we can allow the Taylor expansion of pressure alone to define the whole weather situation. In this respect, the surge analysis is similar in principle to the methods of Doodson (1924), Darbyshire & Darbyshire (1956), Rossiter (1959), and others, who also correlate sea level with pressure gradients or their squares. However, the present analysis is more comprehensive in its treatment of variations in time, and in the inclusion of higher order spacial derivatives of pressure.

As with the tides, the techniques adopted for analysis of surges make free use of the frequency transforms of the time series involved, that is, in their (complex) *spectra*. Spectral analysis can conveniently be done only if long continuous stretches of time series (sea levels, atmospheric pressures, etc.) are available. In fact continuous series covering all of the three years 1959, 1960, 1961 were prepared and used. This approach again differs from that of most workers, who tend to regard storm surges as isolated events lasting only a day or so.

PHILOSOPHICAL TRANSACTIONS OF THE ROYAL SOCIETY A MATHEMATICAL, PHYSICAL & ENGINEERING SCIENCES

Concentration on the most violent disturbances has immediate practical appeal, but the smaller oscillations, which are continually present, even in summer time, are due basically to the same physical mechanisms, and are here treated accordingly.

The final product of the analysis is a set of empirical formulae which could be used to predict sea level at the chosen places a few hours in advance. Apart from their potential utility in flood warning, these formulae are not of great scientific interest in themselves. The principal interest lies in some of the incidental results which emerge in the course of the analysis, and in the techniques themselves, most of which have not previously been applied to tide-gauge records.

The only way to avoid empiricism in surge prediction is to solve the dynamical equations over the whole sea area, either numerically (for example, Hansen 1956), or by electrical analogue (Ishiguro 1962). The response functions used in the 'influence method' of Welander (1961) could also be derived from such computations, but Welander suggests they be determined empirically, making his method somewhat akin to the present one. While many people favour a purely dynamical approach on principle, all the above methods involve more or less rough approximations to the true physical conditions. For example, the effects of irregular coastlines and bottom topography, boundary stresses and nonlinear terms all have to be treated with some compromise. Such approximations are largely avoided in the present method by analysing the record of sea level itself, but are replaced by the uncertainties of statistical estimation. Both empirical and dynamical methods have their faults and advantages. The only reliable test of efficiency is to compare variances or similar measures of their prediction errors. This paper presents a full account of the variances associated with the derived predictions.

2. Theoretical background

The dynamical equations for tides and surges with various degrees of approximation are well known. Charnock & Crease (1957), also Welander (1961), discuss the criteria for neglect of certain terms. Let x, y and z be local Cartesian coordinates with z vertically upwards and u, v and w the corresponding components of velocity. With the mean surface at $z = 0$, the bottom topography is denoted by $z = -h(x, y)$, and the local elevation of the surface at time t by $z = \zeta(x, y, t)$. f, g and ρ denote the Coriolis parameter (latitude dependent), the acceleration due to gravity, and water density, respectively. Using a notation similar to that of Welander (1961), let $\overline{uv}$, for example, denote the *mean value* of the product uv over the local depth of water, from $z = -h$ to ζ strictly, but from $z = -h$ to 0 with sufficient accuracy in many cases. Then the dynamic equations and the equation of continuity can be written approximately as

$$\left.\begin{aligned} \frac{\partial \bar{u}}{\partial t}+\frac{\partial \overline{u^2}}{\partial x}+\frac{\partial \overline{uv}}{\partial y}-f\bar{v} &= -g\frac{\partial}{\partial x}(\zeta-\zeta_g'-\zeta_p')+\frac{1}{\rho h}(\tau_x^w-\tau_x^b),\\ \frac{\partial \bar{v}}{\partial t}+\frac{\partial \overline{uv}}{\partial x}+\frac{\partial \overline{v^2}}{\partial y}+f\bar{u} &= -g\frac{\partial}{\partial y}(\zeta-\zeta_g'-\zeta_p')+\frac{1}{\rho h}(\tau_y^w-\tau_y^b),\\ \frac{\partial \bar{u}}{\partial x}+\frac{\partial \bar{v}}{\partial y} &= -\frac{1}{h}\frac{\partial \zeta}{\partial t}, \end{aligned}\right\} \qquad (2{\cdot}1)$$

where ζ'_g is the equilibrium tide

$$\doteqdot \text{(gravity potential of Moon and Sun†)} \div g,$$

and ζ'_p is the static 'inverted barometer' effect

$$= -\text{(excess of atmospheric pressure over its local mean value)} \div \rho g.$$

τ^w_x, τ^w_y are the x and y components of the surface windstress and τ^b_x, τ^b_y are the x and y components of the bottom stress due to turbulent friction.

In the deep ocean h is large, so the terms involving wind and bottom stress can be neglected, as also the nonlinear terms on the left-hand side of the first two equations, being of order ζ/h compared with the first terms. Then the system is virtually linear, and can in principle be solved for $u(x,y,t)$, $v(x,y,t)$ and $\zeta(x,y,t)$, given appropriate boundary conditions and separate driving functions $\zeta'_g(x,y,t)$ and $\zeta'_p(x,y,t)$. In fact there is little interest in ζ'_p as a driving function over the deep ocean, because atmospheric pressure systems in general move slowly compared with the critical wave velocity $\sqrt{(gh)}$, so that the response there is virtually static. This static response has been confirmed experimentally at Honolulu by Munk & Bullard (1963), but shown to be invalid on continental shelves by Hamon (1966) and in the present paper.

(*a*) *Tidal forces*

The linearized equations, expressed in spherical coordinates with only ζ'_g as driving function, are of course the classic tidal equations of Laplace (Lamb 1932). It would be irrelevant here to discuss their mathematical solutions for idealized oceans of constant depth, or the efforts now in progress to solve them numerically for the actual configurations of the world's oceans. It suffices to say that the latter work involves massive computational problems, and that a realistic solution probably requires the addition of arbitrary dissipative terms to the equations, to account for coupling between surface and internal modes. Here we adopt the empirical approach; assume solutions exist in a reasonable form, and estimate their numerical parameters by analysis of recorded sea levels.

In M.C., a method was given for computing ζ'_g as a function of colatitude θ, east longitude λ, and time, in the form

$$\zeta'_g(\theta,\lambda,t) = \sum_{n=0}^{\infty}\sum_{m=0}^{n}[a^m_n(t)\,U^m_n(\theta,\lambda) + b^m_n(t)\,V^m_n(\theta,\lambda)], \tag{2·2}$$

where

$$U^m_n + \mathrm{i}V^m_n = (-1)^m\left[\frac{2n+1}{4\pi}\right]^{\frac{1}{2}}\left[\frac{(n-m)!}{(n+m)!}\right]^{\frac{1}{2}}P^m_n(\cos\theta)\,\mathrm{e}^{\mathrm{i}m\lambda}, \tag{2·3}$$

a set of complex spherical harmonics. The orthogonal pairs of time series $a^m_n(t)$, $b^m_n(t)$ are computed directly from adequate formulae for the motions of the Moon and Sun. The familiar gravitational effects are defined accurately enough by restricting the first sum in (2·2) to $n = 2$ and 3 only. In order to allow for certain direct and indirect effects on sea level of solar radiation, a *radiation potential* was defined by a similar spherical harmonic series with coefficients $\alpha^m_n(t)$, $\beta^m_n(t)$. (χ^m_n is used to denote $\alpha^m_n + \mathrm{i}\beta^m_n$). For this function the predominant values of n are 1 and 2.

† The full expression (cf. M.C.) includes also the Sun's 'radiation potential'.

Substitution of (2) into the Laplace equations (possibly with some linear damping term), and supposed integration over the real ocean topography, leads generally to a solution for ζ (and for $\bar{u}$ and $\bar{v}$) which at any particular location (θ, λ) is of the form

$$\tilde{\zeta}_{\theta,\lambda}(t) = \mathscr{R} \sum_m \sum_n \int_0^\infty c_n^{m*}(t-\tau)\, R_n^m(\tau)\, \mathrm{d}\tau, \tag{2·4}$$

where $c_n^m(t) = a_n^m + \mathrm{i}b_n^m$ and * denotes the conjugate, $a - \mathrm{i}b$. The impulse response functions $R_n^m(\tau)$ thus express a fixed relation between the predicted tide at the place (θ, λ) and the time series $c_n^m(t)$ representing the equilibrium tide. In practice, the $R(\tau)$ functions are replaced by an equivalent finite set of 'weights' which have the same Fourier transform as $R(\tau)$ over the relevant part of the frequency spectrum of $c(t)$. These weights are estimated by correlation or cross-spectral analysis of $\zeta(t)$ with $\zeta_g'(t)$, by the use of techniques discussed in M.C.

A purely linear representation such as (2·4) was shown in M.C. to be appropriate to sea level at Honolulu, an oceanic island. At a more typical situation the tides have had to travel over part of the continental shelf, so that the nonlinear terms in (2·1) and the part of the bottom stress τ^b due to tidal currents begins to be felt. An appropriate analytical technique, however, would still be to solve the linearized equations to give a first approximation $\zeta = \tilde{\zeta}^{\mathrm{I}}$, then substitute $\tilde{\zeta}^{\mathrm{I}}$ into the nonlinear terms to give a modified driving force in the shallow region. (A reasonable approximation for the relation between $\bar{u}$, $\bar{v}$ and $\overline{uv}$ has to be made.) This yields a second approximation $\tilde{\zeta} = \tilde{\zeta}^{\mathrm{I}} + \tilde{\zeta}^{\mathrm{II}}$ say, where the perturbation $\tilde{\zeta}^{\mathrm{II}}$ is generally of the form (cf. Hasselmann, Munk & MacDonald 1963)

$$\tilde{\zeta}^{\mathrm{II}}(t) = \int_0^\infty \int_0^\infty \tilde{\zeta}^{\mathrm{I}}(t-\tau)\, \tilde{\zeta}^{\mathrm{I}}(t-\tau')\, R(\tau, \tau')\, \mathrm{d}\tau\, \mathrm{d}\tau'. \tag{2·5}$$

Nonlinear bottom friction tends to induce tertiary forms $\tilde{\zeta}^{\mathrm{III}}$, expressible as a triple integral similar to (2·5). Binary and tertiary forms were accommodated in predictions for Newlyn, Cornwall by means of additional sets of weights. In § 3 I show that linear forms with complete perturbations of order 2 and 3 are sufficient for tidal predictions at a wider variety of shallow water ports.

(*b*) *Meteorological forces*

Since the response to ζ_p' over the deep ocean is static, we may regard the meteorological terms in (2·1) as effective only over the local continental shelf. In the present study this means principally the shelf north and west of Ireland and Scotland, and the North Sea. Because of the limited area, it is now fairly reasonable to retain rectangular coordinates. The nonlinear terms are still small except in very shallow areas such as river estuaries, and most computations ignore them altogether. In any case, the efficacy of the tidal analysis outlined in (*a*) confirms that they can be treated as second and third order perturbations to a linear solution.

The bottom stress (τ_x^b, τ_y^b) is essentially a function of the mean (turbulent) current near the bottom. We shall assume for convenience that it can also be expressed as a simple function of the depth-mean current $(\bar{u}, \bar{v})$ appearing in (2·1), although Welander (1961, p. 341) points out some cases near a coastline where this would not be quite true. With the above assumption, the bottom stress terms can be treated (as they usually are) as part of the left-hand side of the equations. The actual form of the frictional law will be discussed in § 4 (*b*).

PHILOSOPHICAL TRANSACTIONS OF THE ROYAL SOCIETY A MATHEMATICAL, PHYSICAL & ENGINEERING SCIENCES

The wind stress (τ_x^w, τ_y^w) is, similarly, a function of the 'surface wind'. If the wind has components (W_x, W_y), the stress is often expressed in the form

$$(\tau_x^w, \tau_y^w) = k\rho_a \sqrt{(W_x^2 + W_y^2)}\,(W_x, W_y), \tag{2·6}$$

where ρ_a is air density and k is an arbitrary factor. k depends somewhat on wind speed and air stability (see, for example, Sheppard 1958), but an average value of $2{\cdot}5 \times 10^{-3}$ is commonly accepted. However, Welander (1961, p. 363) reports some computations on a large surge in the North Sea for which a considerably lower value of k applied, and Darbyshire & Darbyshire (1956) and others have found that a linear wind stress gives as good results as a quadratic law.

Assuming $\zeta_p'(x, y, t)$, $\tau_x^w(x, y, t)$, and $\tau_y^w(x, y, t)$ are defined over the whole sea area, the linearized form of (2·1) can again be solved for $\zeta(t)$ at any place (x, y), analogously to the method discussed in (*a*). There are various possible approaches. In Welander's 'influence method' one divides the sea into a mesh of M elementary areas, at each of which the three stresses are supposed to be defined in time. The sea level ζ at a particular place $Q(x', y')$ is then expressed as the sum of $3M$ impulse-response relations, say

$$\zeta_Q(t) = \sum_{m=1}^{M} \left[\int_0^\infty \zeta_p'^{(m)}(t-\tau)\, R_1^{(m)}(\tau)\, \mathrm{d}\tau + \int_0^\infty \tau_x^{w(m)}(t-\tau)\, R_2^{(m)}(\tau)\, \mathrm{d}\tau + \int_0^\infty \tau_y^{w(m)}(t-\tau)\, R_3^{(m)}(\tau)\, \mathrm{d}\tau \right]. \tag{2·7}$$

This is essentially the same as regarding $\zeta_p'(x, y, t)$, for example, as the sum of M functions each of which is zero everywhere except at one of the M mesh areas.

The method proposed and used in this paper is closer to that used for the tide potentials. $\zeta_p'(x, y, t)$ is expanded in a Taylor series about an origin (55° N, 0° E) in the interior of the sea area, that is,

$$\zeta_p'(x, y, t) = p_{00}(t) + xp_{10}(t) + yp_{01}(t) + x^2 p_{20}(t) + 2xyp_{11}(t) + y^2 p_{02}(t) + \ldots \tag{2·8}$$

The sea level ζ at Q, as affected by normal pressure, can then be expressed as the sum of responses to the series of coefficients $p_{ij}(t)$, that is

$$\zeta_Q(t) = \sum_{i,j} \int_0^\infty p_{ij}(t-\tau)\, R_{ij}(\tau)\, \mathrm{d}\tau. \tag{2·9}$$

A similar process could be applied to the wind stress components, but it is clearly an advantage to use its relation to the geostrophic wind, which is proportional to the pressure gradients already defined in (2·8).

The relation between geostrophic and surface winds is not too well understood, but an average reduction factor and change of direction at any latitude is usually adequate (Dietrich *et al.* 1952). At the origin, for example, formulae such as $W_x = \mathrm{A}p_{10} + \mathrm{B}p_{01}$, $W_y = \mathrm{C}p_{10} + \mathrm{D}p_{01}$, with A, B, C, D known constants, can therefore be assumed. Some may prefer to use the 'gradient wind', which involves the radius of curvature of the isobars as well as their gradients. However, to express this numerically in terms of the pressure field $\zeta_p'(x, y, t)$ requires awkward nonlinear terms, and Rossiter (1959) and others have found that it yields no improvement in surge analysis. As a final compromise, we assume a linear relationship between surface wind and stress, so that (τ_x^w, τ_y^w) is assumed to depend linearly

on the pressure gradients. In view of the many uncertainties involved it would seem difficult to improve on this assumption very significantly.

The great advantage of the above assumption is that the expansion (2·8) can be taken to represent the wind stress as well as the normal pressure. The responses $R_{ij}(\tau)$ to the coefficients $p_{ij}(t)$ can, if estimated empirically, be taken to define the entire linear response of the sea level to the meteorological forces. The fact that available records of atmospheric pressure are more reliable than those of wind speed adds to the advantages. The coefficients in (2·8) are quite easily derived from records of pressure at suitably spaced fixed stations.

(c) *Frequency transforms*

As in M.C., it is found useful to work in terms of the frequency (Fourier) transforms of all time series and response functions. Let $\gamma^j(t)$ be one of the driving functions (tidal or meteorological), and $G^j(f)$ its transform or *spectrum*,

$$G^j(f) = \int_{-\infty}^{\infty} \gamma^j(t)\, \mathrm{e}^{2\pi \mathrm{i} f t} \mathrm{d}t.$$

If $\zeta^j(t)$ represents that part of the total sea level variation $\zeta(t)$ due to the driving force $\gamma^j(t)$, then the response relation

$$\zeta^j(t) = \int_0^{\infty} \gamma^j(t-\tau)\, R^j(\tau)\, \mathrm{d}\tau$$

is equivalent to expressing that the spectrum of $\zeta^j(t)$ is

$$H^j(f) = Z^j(f)\, G^j(f)$$

where $Z^j(f)$ is an *admittance* function equal to the transform of $R^j(\tau)$. Thus,

$$Z^j(f) = \int_0^{\infty} R^j(\tau)\, \mathrm{e}^{2\pi \mathrm{i} f \tau}\, \mathrm{d}\tau,$$

and a similar reciprocal relation holds. The relevant admittance $Z^j(f)$ can be estimated by cross spectral analysis of $\zeta(t)$ and $\gamma^j(t)$ as outlined below.

Like $R^j(\tau)$, $Z^j(f)$ completely defines the linear relation between $\gamma^j(t)$ and $\zeta^j(t)$. Its advantages are that it enables one to separate tidal and nontidal parts of the spectrum, and that its form gives a useful guide to the choice of the time interval $\Delta\tau$ and number of terms S necessary to represent $R^j(\tau)$ in the discrete form $(R^j(s\Delta\tau),\ s = O(1)\, S)$. In some cases, particularly for the tides, the admittance $Z(f)$ is more meaningful than the discrete set of response weights $R(s\Delta\tau)$.

In practice, with given time series at interval Δt, I have used the following discrete estimates of the spectra with bandwidth $\Delta f = 1/N\Delta t$:

$$\left.\begin{aligned} G^j_\tau &= N^{-1} \sum_{n=-N}^{N} (1+\cos \pi n/N)\, \mathrm{e}^{2\pi \mathrm{i} r n/N} \gamma^j(n\Delta t - t_0), \\ H_r &= N^{-1} \sum_{n=-N}^{N} (1+\cos \pi n/N)\, \mathrm{e}^{2\pi \mathrm{i} r n/N} \zeta(n\Delta t - t_0) \qquad (r = 1, 2, 3, \ldots, (\tfrac{1}{2}N-1). \end{aligned}\right\} \quad (2\cdot10)$$

In most cases $N\Delta\tau$ was $29\frac{1}{2}$ days, so Δf was less than 1 cycle/month (c/m). The first bracket in each sum eliminates sideband effects from tidal to nontidal parts of the spectrum. Ensemble averages from a series of time origins t_0, denoted by $\langle\ \rangle$, are then taken as estimates of:

the energy spectrum of sea level, $\quad E_r = \langle \tfrac{1}{2} H_r H_r^* \rangle$

the cross spectrum of sea level and function

$$C_r^j + \mathrm{i}Q_r^j = \langle \tfrac{1}{2} G_r^j H_r^* \rangle$$

and the cross spectrum of functions γ^j and γ^k,

$$C_r^{jk} + \mathrm{i}Q_r^{jk} = \langle \tfrac{1}{2} G_r^j G_r^{k*} \rangle.$$

In a simplified case, where $\gamma^j(t)$ is assumed to be uncorrelated with the other driving forces, the appropriate unbiased estimate of the admittance $Z^j(f)$ at frequency $f = r\Delta f$ is simply (see M.C.)

$$Z_r^j = X_r^j + \mathrm{i}Y_r^j = (C_r^j + \mathrm{i}Q_r^j)/C_r^{jj}.$$

However, the pressure coefficients in (2·8) are not independent, so we have to use the more general relation for k driving functions (here we omit the frequency suffix r for convenience, and note that $(C^{kj} = C^{jk},\ Q^{kj} = -Q^{jk})$:

$$\begin{bmatrix} C^{11} & C^{12} & \dots & C^{1k} & 0 & Q^{12} & \dots & Q^{1k} \\ C^{21} & C^{22} & \dots & C^{2k} & Q^{21} & 0 & \dots & Q^{2k} \\ \vdots & \vdots & & \vdots & \vdots & \vdots & & \vdots \\ C^{k1} & C^{k2} & \dots & C^{kk} & Q^{k1} & Q^{k2} & \dots & 0 \\ 0 & Q^{21} & \dots & Q^{k1} & C^{11} & C^{21} & \dots & C^{k1} \\ Q^{12} & 0 & \dots & Q^{k2} & C^{12} & C^{22} & \dots & C^{2k} \\ \vdots & \vdots & & \vdots & \vdots & \vdots & & \vdots \\ Q^{1k} & Q^{2k} & \dots & 0 & C^{1k} & C^{2k} & \dots & C^{kk} \end{bmatrix} \begin{bmatrix} X^1 \\ X^2 \\ \vdots \\ X^k \\ Y^1 \\ Y^2 \\ \vdots \\ Y^k \end{bmatrix} = \begin{bmatrix} C^1 \\ C^2 \\ \vdots \\ C^k \\ Q^1 \\ Q^2 \\ \vdots \\ Q^k \end{bmatrix}. \tag{2·11}$$

The *predictable variance*, $(\text{p.v.})_r$ per frequency bandwidth for the set of k functions, by which is meant the reduction in variance of sea level when the relevant prediction is subtracted from it, is computed from the solution to equations (2·11) by means of the formula

$$(\text{p.v.})_r = \frac{2}{3} \sum_{j=1}^{k} (X_r^j C_r^j + Y_r^j Q_r^j). \tag{2·12}$$

(The factor $\frac{2}{3}$ is necessitated by the cosine taper in (2·10)). In the limit of infinite statistical samples, the total predictable variance, t.p.v., would equal the sum of the $(\text{p.v.})_r$ values over the spectral range of r. But in practice, since the final sequence of response weights $R^j(s\Delta\tau)$ represents a smoothed admittance function through the scattered sequence of estimates Z_r^j, t.p.v. is somewhat less than $\Sigma(\text{p.v.})_r$.

(*d*) *Surge-tide interaction* (*theory*)

In (*a*) and (*b*) we have considered linear and nonlinear representation of tides but only the linearized surge response. The second order perturbation will again be expressed as a double integral similar to (2·5), which will ideally contain the products

$$\zeta_T^{\mathrm{I}}(t-\tau)\,\zeta_S^{\mathrm{I}}(t-\tau') \quad \text{and} \quad \zeta_S^{\mathrm{I}}(t-\tau)\,\zeta_S^{\mathrm{I}}(t-\tau'),$$

where the suffixes T and S refer to tide and surge respectively. We shall ignore the second type, which may be described as the interaction of the surge with itself, because it is in general too small to be isolated by the analytical method of this paper. The interaction of surge and tide was itself ignored in most early papers, but experience with surge predictions has shown its importance in shallow water areas. Recently it has been receiving more

attention, analytically (Proudman 1957) and by digital computation (Rossiter 1961), but I have not seen any published account of its explicit inclusion in an empirical formula for surge prediction.†

In the present study a surge-tide interaction response function $R_{ST}(\tau, \tau')$ is again evaluated from its frequency transform $Z(f_1, f_2)$, which may be termed a 'bi-admittance', or 'interaction coefficient'. The work is simplified by the dominance of the semi-diurnal tide, which enables f_2 to be fixed at about 2 c/d. For purposes of analysis, I have taken the actual nontidal sea level, rather than some form of linear prediction, to represent the surge. The interaction coefficients $Z(f_1, f_2)$ are then closely related to the bispectrum (Hasselmann *et al.* 1963) of the sea level itself, without reference to external forces. Indeed, the spectral analysis plays an essential part in separating the tidal and nontidal elements.

There is, however, a certain ambiguity to overcome. Let $H_{r_1}, H_{r_2}, H_{r_3}$ be spectral elements of sea level (2·10), where r_1 corresponds to an arbitrary nontidal frequency $2\pi r_1 \Delta f$, r_2 to the principal semi-diurnal frequency at 2 c/lunar day (c/l.d.) and $r_3 = r_2 - r_1$, which for convenience we may assume positive. H_{r_3} contains an element h_3 which is coherent with the interaction between H_{r_1} and H_{r_2}, and also a residual element h_3', uncorrelated with h_3. Similarly, $H_{r_1} = h_1 + h_1'$, where h_1 is due to the interaction between H_{r_3} and H_{r_2}. That is,

$$h_3 = Z(-f_1, f_2)\, H_{r_1}^* H_{r_2}$$

and

$$h_1 = Z(-f_3, f_2)\, H_{r_3}^* H_{r_2},$$

where f_k are the frequencies, proportional to the harmonic numbers r_k. By analogy with the procedure for estimating a linear admittance $Z(f)$, we consider the ensemble average of the product

$$(H_{r_1}^* H_{r_2})\, H_{r_3}^* = (H_{r_3}^* H_{r_2})\, H_{r_1}^* = H_{r_1}^* H_{r_3}^* H_{r_2},$$

whose expected value is found, by setting incoherent products to zero, to be

$$H_{r_2} H_{r_2}^* [Z(-f_1, f_2)\, h_1' h_1'^* + Z(-f_3, f_2)\, h_3' h_3'^*]. \tag{2·13}$$

Since there is no special relation between the two values of Z, (2·13) is useful only when one of the two quantities in square brackets is much larger than the other. This is the case for the range

$$-0{\cdot}5 \text{ c/d} \leqslant -f_1 \leqslant +1{\cdot}6 \text{ c/d}$$

because the energy spectrum of sea level here is very much greater than in the nontidal part of the corresponding range

$$1{\cdot}5 \text{ c/d} \leqslant f_3 \leqslant 3{\cdot}6 \text{ c/d}.$$

At these frequencies, we can then assume

$$Z(-f_1, f_2) \approx \langle H_{r_1}^* H_{r_3}^* H_{r_2} \rangle / \langle |H_{r_2}|^2 |H_{r_1}|^2 \rangle. \tag{2·14}$$

The estimator for the bispectrum itself (with one variable f_2 fixed), is the numerator of the right-hand side of this equation. The *bicoherence*

$$|\langle H_{r_1} H_{r_3} H_{r_2}^* \rangle|^2 / \langle |H_{r_1}|^2 |H_{r_2}|^2 |H_{r_3}|^2 \rangle,$$

has the same sort of meaning as a conventional coherence coefficient.

† The U.K. 'Storm Tide Warning Service' are experimenting with linear prediction formulae restricted to times of high tide; these must contain some implicit form of interaction.

To the values of $Z(f_1, f_2)$ obtained from the above process I add the isolated values from the pure tidal analysis, thus extending the range of f_1 to -2 to $+2$ c/l.d. A Fourier series of period 8 c/d fitted to all values (weighted according to their bicoherences), expresses the frequency transformation

$$Z(f_1, f_2)\ (-2 \leqslant f_1 \leqslant 2, f_2 = 2\,\text{c/l.d.}) = \sum_{s=0}^{S} R(s, 0)\, \mathrm{e}^{-2\pi \mathrm{i} f s \Delta\tau} \tag{2·15}$$

where $\Delta\tau = 3$ h, and S is chosen as large as necessary. With the discrete set of response weights R defined by (2·15), the bilinear surge-tide interaction then takes the form

$$\tilde{\zeta}^{\mathrm{II}}_{ST}(t) = 2 \sum_{s=0}^{S} R(s, 0)\, \tilde{\zeta}^{\mathrm{I}}_{S}(t - s\Delta\tau)\, \tilde{\zeta}^{\mathrm{I}*}_{T}(t), \tag{2·16}$$

where $\tilde{\zeta}^{\mathrm{I}}_{S}$ is the linear predicted surge, and $\tilde{\zeta}^{\mathrm{I}}_{T}$ is the predicted *semi-diurnal* tide.

The tertiary interaction involving $\zeta_S \zeta_T \zeta_T$ is treated by evaluating two further sets of weights $R^{+}(s, 0, 0)$ and $R^{-}(s, 0, 0)$, associated with bilinear tidal functions $(\tilde{\zeta}^{\mathrm{I}}_{T})^2$ and $(\tilde{\zeta}^{\mathrm{I}}_{T} \tilde{\zeta}^{\mathrm{I}*}_{T})$ respectively.

3. Preparation of data

The geographical positions of the places from which sea levels and atmospheric pressures were obtained are shown in figure 1. Their names, latitudes and longitudes are listed in table 1.

Table 1. Recording stations

place	latitude	longitude	data	
Malin Head	55° 23′ N	7° 24′ W	sea level	pressure
Stornoway	58° 12′ N	6° 23′ W	sea level	pressure
Lerwick	60° 09′ N	1° 09′ W	sea level	pressure
Aberdeen (Pocra)	57° 09′ N	2° 05′ W	sea level	—
Aberdeen (Dyce)	57° 12′ N	2° 11′ W	—	pressure
Immingham Dock	53° 38′ N	0° 11′ W	sea level	—
Spurn Head	53° 36′ N	0° 07′ E	—	pressure
Southend Pier	51° 31′ N	0° 44′ E	sea level	—
Gorleston	52° 36′ N	1° 43′ E	—	pressure
Noord Hinder	51° 39′ N	2° 34′ E	—	pressure
Terschellinger	53° 29′ N	5° 08′ E	—	pressure

The tide gauge data for Malin Head were supplied in the form of hourly lists by the Irish Ordnance Survey, Dublin. Those for Stornoway and Lerwick were from gauges installed by the National Institute of Oceanography. Data for Aberdeen, Immingham and Southend were read off tide gauge charts obtained from the respective port authorities. Atmospheric pressures for all places except the last two were obtained every 3 h from the Daily Weather Reports issued by the Meteorological Office. Those for Noord Hinder and Terschellinger Bank (both lightships) were obtained every 6 h from the annual publications of the Royal Netherlands Meteorological Institute, De Bilt.

The period chosen was the longest possible time during which data from all places were reasonably reliable and continuous. This was limited by the tide gauge at Stornoway to 1 January 1959–2 January 1962, a total of 1098 days. The only lacunas were a 5 week period in the Malin sea levels in May–June 1960, a 2 week period at Southend in August 1960, and

a few gaps of 1 to 3 days in various other sea level records. The two large gaps mentioned were filled by conventional tide predictions, which, being for summer time, were probably fairly accurate, and those of 1 to 3 days by suitable interpolations. The meteorological data were practically complete, except for a very few isolated missing values which were easily interpolated.

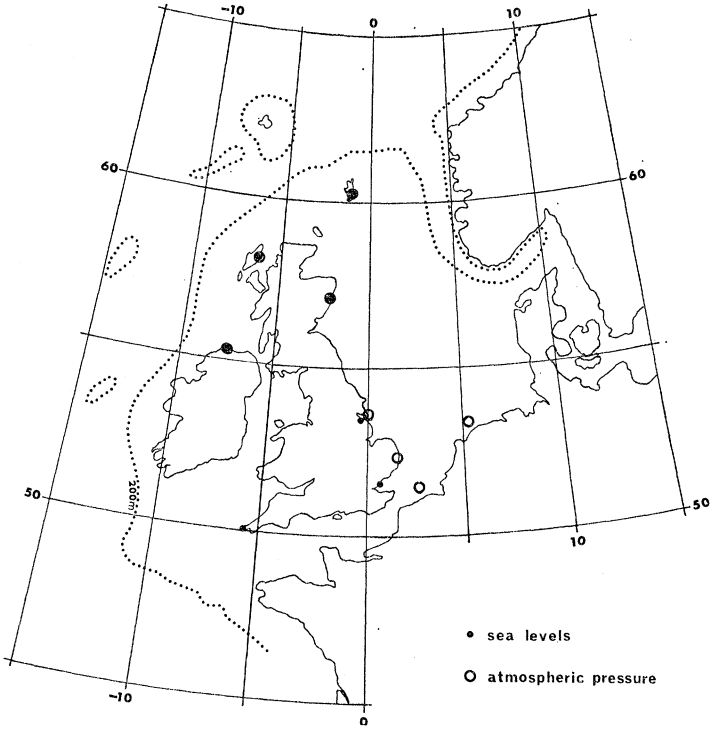

FIGURE 1. The north west European continental shelf. ●, Sea level station; ○, atmospheric pressure station. The dotted line represents the 200 m depth contour.

All hourly sea levels were subjected to the following smoothness test by computer. For each n, the X_n was compared with

$$X'_n = 0{\cdot}75(X_{n+1}+X_{n-1})-0{\cdot}30(X_{n+2}+X_{n-2})+0{\cdot}05(X_{n+3}+X_{n-3}).$$

The difference $(X_n-X'_n)$ is zero for any quintic polynomial, and an isolated large error produces a recognizable symmetrical sequence of differences. All differences with magnitude greater than 0·3 ft. (the least count was 0·1 ft. in all cases) were listed by the computer. The lists were then checked by human intelligence and the data corrected where necessary. This scheme was found preferable to a checking procedure in common use, whereby the computer inserts an interpolated value whenever a specified difference is exceeded. The chief reasons are, first, that some departures from smoothness are inherent in the data (commonly just after low-water springs at a shallow water port), and secondly, that the genuine errors can take too many different forms (for example, a sequence of several values all read 1 h late) to be conveniently embodied in a computer program. In short, to detect errors some human judgement is considered necessary.

For the comparative analysis of sea level and weather, and also for the analysis of tides of species 1 to 3, the corrected sea level series were smoothed to a 3 h time interval by means

of a standard low pass filter† with cutoff at 4 c/d and amplitude response between 0·999 and 1·001 for the frequency range 0 to 3·6 c/d. (In the range of the semi-diurnal tides the response lay between 0·99998 and 1·00002.) Application of the filter absorbed the first and last $2\frac{1}{2}$ days of data, so the final length of the 3 h sea level series was 1093 days. This is a convenient period for tidal analysis, since 1093 days equals 40·0050 tropical months or 2·9925 tropical years.

The meteorological data were passed through a similar though slightly less rigorous test for errors. After correcting,‡ the 6 h Netherlands data were expanded to a 3 h series by means of the interpolation

$$p(t) = \tfrac{9}{16}[p(t+3)+p(t-3)]-\tfrac{1}{16}[p(t+9)+p(t-9)] \qquad (3{\cdot}1)$$

for uniformity with the other pressure series. A test of (3·1) applied to the 3 h pressures at Gorleston during January 1959 gave a standard error of 0·57 mb.

The mean pressures over the 3 y period varied between 1009·8 mb at Stornoway and 1014·3 mb at Gorleston, with a rough gradient of −0·5 mb per degree of latitude. The overall average of 1012·0 mb was subtracted from all the data.

4. Analysis of tides

(*a*) *Species* 1, 2, 3

Following the reasoning and experience of M.C., the response weights for the first three tidal species for all six ports were evaluated from the matrix of covariances between sea levels and the appropriate potential functions, for the 1093 day 3 h series referred to in § 3. The period was long enough for covariances between different tidal species to be considered as zero.

Computations for the low frequency (species 0) tides were omitted, partly because the signal: noise ratio is here too low to obtain significant results with 3 y data, and also because the whole low frequency variation was later treated by self-prediction (see § 8). Section 9 describes some results on the monthly and fortnightly tides, derived after using the weather variables to reduce the noise level.

The selected tidal variables are listed in table 2, and their respective weights (P, Q) in the appendix. The gravity and radiation potentials were computed exactly as described in M.C., but, because of the shorter span of data, I have used fewer variables and time lags than for the 19 y analyses. The radiation potentials χ_1^1 and χ_2^1 are omitted because the diurnal energy is generally weak, and their effect on the 19 y analysis for Newlyn was hardly noticeable. The cusp-forming product of tide potential and local mean sea level, $\overline{\zeta} c_n^m$, is omitted for similar reasons; its insignificance is confirmed in § 4 (*c*).

All nonlinear terms are accommodated by means of products of first order predictions for species 1 and 2, $\tilde{\zeta}_1^1$ and $\tilde{\zeta}_2^1$ respectively (see M.C., p. 564). These require fewer time lags, besides giving more meaningful interaction weights, which I use in § 5. However, $\tilde{\zeta}_1^1$ and $\tilde{\zeta}_2^1$ themselves require a set of weights to be derived by an initial pilot analysis in terms of lagged

† Bullard *et al.* (1966), pp. 41–46, give an excellent summary of filter characteristics. The filter referred to here used the parameters $c = 5$, $m = 61$, $f = \frac{1}{3}$.

‡ The detected errors were in the transferred data, not in the original publication.

variables c_2^1, c_2^2 only. (These weights can also be deduced from the major harmonic constituents, if known previously.) The weights derived and used here are listed separately in the appendix.

TABLE 2. VARIABLES USED FOR ALL PORTS

$c_n^m(S)$ refers to the tidal potentials (2·2) with time lags between $\pm S$, i.e. $2S+1$ lags. $\zeta^{j\pm k}$ refers to interaction products $\tilde{\zeta}_j^{\mathrm{I}}\tilde{\zeta}_k^{\mathrm{I}}$ or $\tilde{\zeta}_j^{\mathrm{I}}\tilde{\zeta}_k^{\mathrm{I}*}$.

tidal species	response method: linear	response method: nonlinear	no. of pairs	harmonic method	no. of pairs
1	$c_2^1(2)$, $c_3^1(0)$	$\zeta^{2-1}\,\zeta^{2-2+1}$	8	$2Q_1$, Q_1, O_1, M_1, P_1, S_1, K_1, J_1	8
2	$c_2^2(2)$, $c_3^2(0)$, $\chi_2^2(0)$	ζ^{2-2+2}	8	$2N_2$, μ_2, N_2, ν_2, M_2, L_2, T_2, S_2, K_2, MNS_2, $2SM_2$	11
3	$c_3^3(1)$	$\zeta^{2+1}\,\zeta^{2+2-1}$	5	$2MK_3$, M_3, SO_3, MK_3, SK_3	5
4		ζ^{2+2} (0, 0), (0, 1), (1, 1)	3	MN_4, M_4, MS_4, MK_4, S_4	5
5		ζ^{2+2+1}	1		0
6		ζ^{2+2+2}	1	$2MN_6$, M_6, MSN_6, $2MS_6$, $2SM_6$	5

Time lags are used only for the principal convolutions, in the form:

$$\mathscr{R}\sum_{s=-S}^{S} R_s\, c_2^{m*}(t-s\Delta\tau) = \sum_{s=-S}^{S}[P_s a_2^m(t-s\Delta\tau)+Q_s\, b_2^m(t-s\Delta\tau)], \tag{4·1}$$

where $\Delta\tau = 2$ days, chosen so that $\Delta\tau^{-1}$ is twice the bandwidth of the 'input spectrum' of c_2^m, and $S \leqslant 3$, (M.C., pp. 544–545). For species 1 ($m=1$), S was restricted to 2, but for the important species 2 input c_2^2 the 7-term summation given by $S=3$ was also investigated. Table 3 shows a typical comparison of the weights derived for c_2^2 with $S=2$ and 3 from the sea level record at Stornoway. The large coefficients in the 7-term set indicate 'over fitting'. Their corresponding admittance function

$$Z(f) = \sum_{s=-S}^{S} R_s\, \mathrm{e}^{-2\pi \mathrm{i} f s\Delta\tau} \tag{4·2}$$

sums to appropriate values within the spectral bandwidth, but oscillates widely outside. The sum ΣR_s, given at the foot of the table, being in fact $Z(f)$ at the solar frequency $f = 2$ c/d, is a useful indication of the true magnitude of the admittance. The danger is that the large oscillations in $Z(f)$ may unduly magnify some minor spectral component in c_2^2, or allow, for example, the radiation weights to take distorted values.† The whole situation is much more comfortable in the 5-term set shown on the right, and this applied at all ports.

This result perhaps reflects adversely on the choice of a 7-lag set of weights for Newlyn in M.C. However, none of the Newlyn weights exceeds in magnitude $10\,|Z(2)|$ as do

† The difference in ΣQ_s in the two cases is in fact balanced by a substantial difference in the estimated radiation weights.

several values on the left of table 2. It seems probable that the longer period of analysis allows a more extended set of variables to be used without undue over-fitting, by reducing the sampling errors.

TABLE 3. 7-TERM AND 5-TERM SETS OF WEIGHTS FOR STORNOWAY

s	P	Q	P	Q
3	7·3	−5·0	—	—
2	−32·5	−7·6	1·2	−0·1
1	34·8	52·3	−2·4	−1·5
0	8·0	−72·3	−2·6	4·5
−1	−43·1	37·3	3·5	−0·9
−2	28·7	1·4	−1·0	−0·7
−3	−4·4	−5·7	—	—
sum	−1·1	0·4	−1·3	1·3

Much of the justification for the method depends on the linear admittances as defined by (4·2) being smooth functions of frequency. In figure 2 are plotted all the functions

$$\ln Z(f) = \ln |Z| + \mathrm{i}(\arg Z)$$

derived from the sets of weights listed in the appendix for the leading linear potentials c_2^1, c_2^2 and c_3^3. The logarithm was chosen so that local magnifications and phase shifts merely move the curves up or down without altering their general shape. With some allowance for inaccuracy at the limits of the spectral bands, the curves confirm the required smoothness, and show a satisfactory conformity from one port to another. The strong decrease with frequency of both phase and amplitude of the diurnal admittance is particularly well preserved, despite the low signal: noise ratio for the species 1 tides. In contrast, the species 2 admittances are fairly flat, although there is also a decrease in phase lead of about 10 rad $(\mathrm{c/d})^{-1}$.

The species 3 admittances for Malin, Stornoway and Lerwick are fairly consistent with each other and with Newlyn (bottom curves), but a dip in magnitude and a phase change at 2·89 c/d develops in the three North Sea ports of Aberdeen, Immingham and Southend. Unfortunately, since the principal lunar ter-diurnal frequency is 2·898 c/d, this is probably due to maladjustment of the nonlinear terms, which get progressively stronger from Aberdeen to Southend. However, the corresponding tide predictions are all quite good, as will be shown later, and rather little energy is involved anyway.

Little need be said about the weights for the remaining linear potentials of degree 3, namely c_3^1 and c_3^2. As for Honolulu and Newlyn, they have about the same order of magnitude as, but no special relation in phase to the admittances of degree 2. The constant admittances implied by the absence of time lags are of course a compromise.

One of the surprising results of M.C. was that the radiational 2 c/d term at Newlyn had an amplitude of 19 cm, about one-third of the total S_2 constituent. Table 4 compares the amplitude and phase of the present radiational components with those of the *linear* gravitational components at 2 c/d. Corresponding results for Newlyn and Honolulu are also included. Earlier spectral analyses showed that the respective amplitudes are 0·557 $|Z(2)|$ cm and 29·5 $|Z(2)|$ cm, where in the first case $Z = P + \mathrm{i}Q$ (for χ_2^2), and in the second,

$$Z = \Sigma P + \mathrm{i}\Sigma Q \quad (\text{for } c_2^2).$$

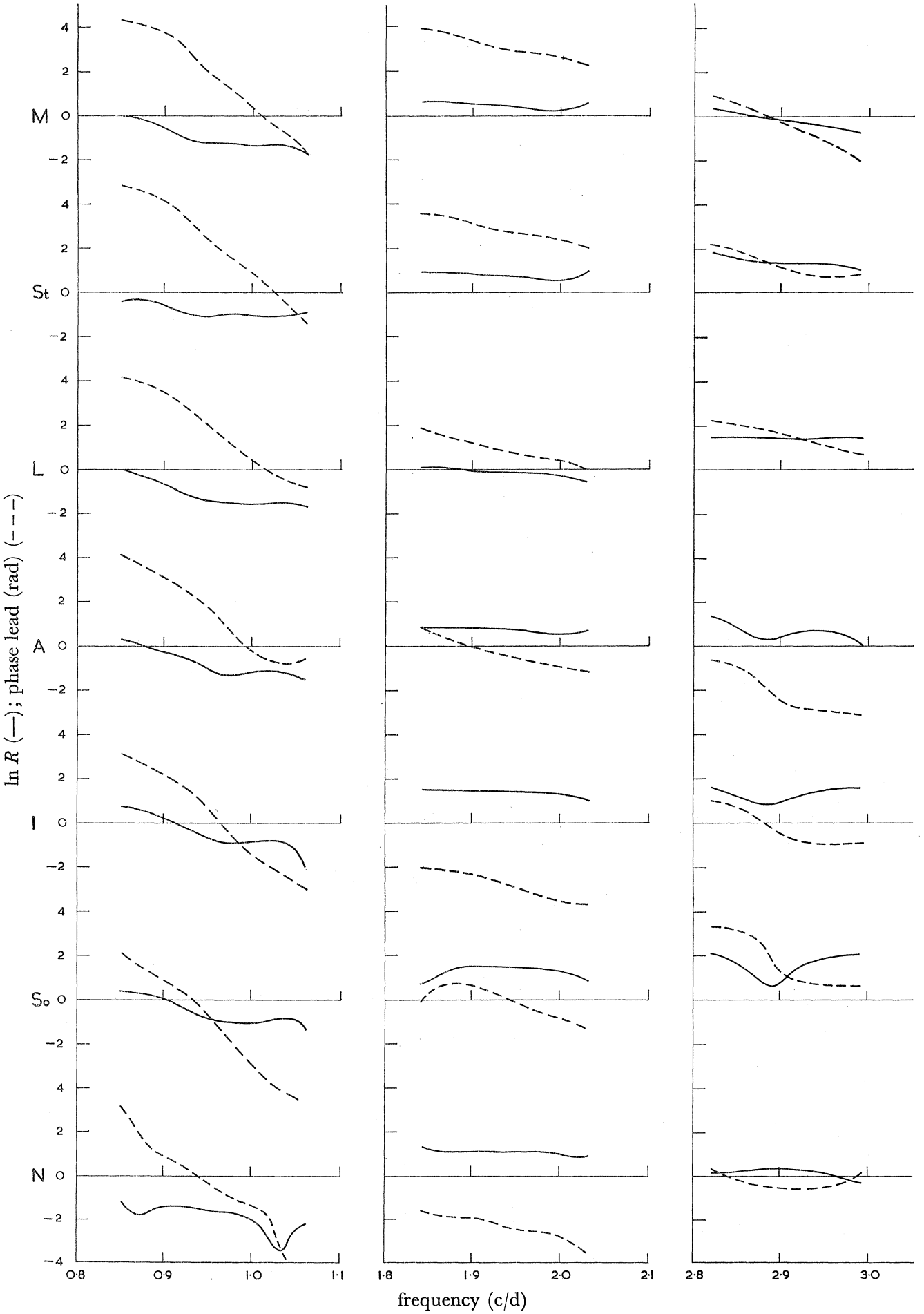

FIGURE 2. Linear admittances (——, ln R; – – –, phase lead (rad)) to the gravitational tide potential coefficients c_2^1, c_2^2 and c_3^3. The six principal ports and Newlyn are denoted by initial letters (St = Stornoway, So = Southend).

PHILOSOPHICAL TRANSACTIONS OF THE ROYAL SOCIETY A MATHEMATICAL, PHYSICAL & ENGINEERING SCIENCES

This is more relevant than a comparison with the total S_2 constituent, since the latter is often distorted by nonlinear effects. From the penultimate line, we see that the amplitude ratio for Newlyn is thereby reduced from 0·33 to 0·23.

TABLE 4. LINEAR COMPONENTS AT 2 C/D

	radiational		gravitational			
place	amplitude (cm)	phase (deg)	amplitude (cm)	phase (deg)	ampl. (rad.) ÷ ampl. (grav.)	phase (rad.) − phase (grav.)
Malin	6·2	90	37·2	153	0·17	297
Stornoway	8·4	43	53·2	136	0·16	267
Lerwick	4·4	253	23·3	23	0·19	230
Aberdeen	5·6	192	50·9	305	0·11	247
Immingham	16·1	340	110·1	158	0·15	182
Southend	18·6	106	109·0	312	0·17	154
Newlyn	18·6	46	81·2	198	0·23	208
Honolulu	1·3	215	5·6	315	0·24	260

The radiational amplitudes vary roughly in proportion to the gravitational amplitudes with an average ratio of 0·18, which is quite substantial. The estimates of phase difference vary between 154 and 297° with an average value 231°. This phase difference accords with the hypothesis that the radiational tide is mainly caused indirectly, by the action of the atmospheric tide on the sea surface, since the tidal atmospheric pressure is minimum 8 h (240°) before the Sun's meridional transit. The ratio of the amplitudes of the atmospheric tide (in centimetres of water) and of the solar equilibrium tide is of order 0·1, which is again comparable with the figures in table 4. However, a full comparison along these lines would require analysis of tides in many sea areas and of the (known) global distribution of the atmospheric tide.

(*b*) *Species* 4, 5 *and* 6

Neglecting the minute linear input to species 4, and interactions of order greater than three, species 4, 5 and 6 are almost entirely due to the interaction products:

$$\tilde{\zeta}^{\mathrm{I}}_2\tilde{\zeta}^{\mathrm{I}}_2, \quad \tilde{\zeta}^{\mathrm{I}}_2\tilde{\zeta}^{\mathrm{I}}_2\tilde{\zeta}^{\mathrm{I}}_1 \quad \text{and} \quad \tilde{\zeta}^{\mathrm{II}}_2\tilde{\zeta}^{\mathrm{I}}_2\tilde{\zeta}^{\mathrm{I}}_2,$$

respectively. Since there are so few input variables to separate, the analysis was confined to the first 355 days of the original hourly data.

Definition in terms of $\tilde{\zeta}^{\mathrm{I}}_m$ rather than of c^m_2 would be expected to require fewer time lags, as was indeed found in the case of species 4 at Newlyn. Nevertheless, some lagged variables such as

$$\tilde{\zeta}^{\mathrm{I}}_2(t-s_1\,\Delta\tau)\,\tilde{\zeta}^{\mathrm{I}}_2(t-s_2\,\Delta\tau)$$

were included in the analysis in order to see if they gave any marked improvement over the case $s_1 = 0, s_2 = 0$. For this purpose $\Delta\tau$ was taken as 1 day, instead of the 2 days used for the linear analysis, and only combinations of 0's and 1's for the s values. Improvements in prediction variances were trivial for species 5 and 6, but considerable for species 4. The greatest improvement was for Stornoway, where the unlagged variable gave 37 cm^2 and the combinations $(s_1, s_2) = (0, 0), (0, 1), (1, 1)$ gave 47 cm^2. This implies that the double interaction is strongly dependent on frequency, even within the band of the semi-diurnal tides.

If two (complex) spectral components ζ_1, ζ_2 at frequencies f_1 and f_2 interact to form components

$$Z(f_1, f_2)\,\zeta_1\,\zeta_2 \quad \text{and} \quad Z(-f_1, f_2)\,\zeta_1^*\,\zeta_2$$

at frequencies (f_2+f_1) and (f_2-f_1) respectively, then as discussed in § 2 (d) we define $Z(f_1, f_2)$ to be the interaction coefficient, or 'biadmittance' of the system. Figure 3 shows the magnitudes and phases of the coefficients of interaction between the M_2 tidal component and

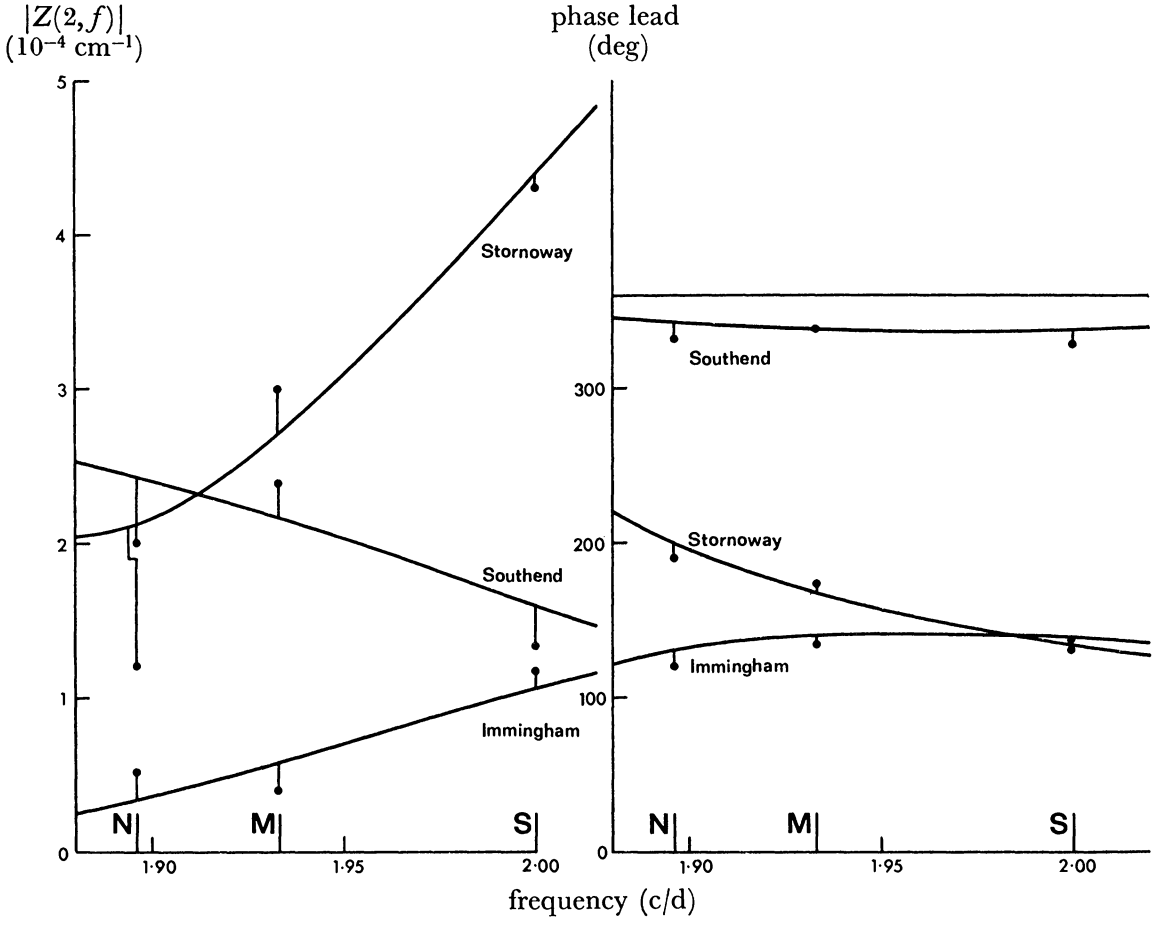

FIGURE 3. Interaction coefficients between the M_2 tide and species 2 tides in general, as function of their frequency. The left-hand diagram shows $|Z(2,f)|$, and the right diagram shows the phase lead in degrees. The curves are computed from the response weights, and the black circles from published harmonic constituents.

components at any other frequency in the same species band for the three ports with the most pronounced species 4 tides. The curves are derived from the transformation formula

$$Z(f_1, f_2) = R_{00} + \tfrac{1}{2}R_{10}\,e^{-2\pi i f_1 \Delta\tau} + \tfrac{1}{2}R_{10}\,e^{-2\pi i f_2 \Delta\tau} + R_{11}\,e^{-2\pi i (f_1+f_2)\Delta\tau}, \qquad (4{\cdot}3)$$

where $\Delta\tau = 1$ day, R_{jk} are the weights for the lag pair $s_1 = j\Delta\tau$, $s_2 = k\Delta\tau$, and the frequency f_2 is fixed at 2 c/l.d. For direct comparison, the black circles represent the values derived from recent lists of harmonic constituents. Thus, for example, at 2 c/d, the magnitude and phase of the interactions are represented by

$$H_{MS_4}/(2H_{M_2}H_{S_2}) \quad \text{and} \quad (-g_{MS_4}+g_{M_2}+g_{S_2})$$

respectively, in standard notation. The black circles do not lie exactly on the curves, partly because more than one pair of primary components can produce a given secondary component (for example, (N_2, L_2) and (μ_2, S_2) also combine to give M_4), but they confirm their general trend fairly well. It is clear from the figure why a constant biadmittance would give inadequate results, but it is remarkable what a variety of trends can occur at different ports in this narrow frequency range. However, it is noteworthy that the *phase* of the biadmittance, but not its magnitude, is nearly constant at Immingham and Southend. The biadmittances will be explored further in § 5.

The triple interaction producing species 5 tides has weights of the same order as those producing species 6, but since the diurnal element is so weak, their associated energy is trivial, and so the weights may not be very reliable. (Zetler & Cummings (1967) have shown that species 5 energy is appreciable at Anchorage, Alaska, where the diurnal tide is considerably greater.)

Both interaction weights and total energy (see table 5) in the species 6 band are large at the shallow water stations Immingham and Southend. Inclusion of time-lags gave almost no improvement in predictable variance, implying a virtually constant admittance over the frequency band. However, another sort of complication has to be considered. In the perturbation expansion of the solution to the shallow water equations (such as the first equation of (2·1)) without friction or other external stresses, if the first approximation is a pure semi-diurnal tide $a_2 e^{2i\omega t}$, we expect subsequent approximations to be of the form

$$a_2 e^{2i\omega t} + a_4 e^{4i\omega t} + a_6 e^{6i\omega t} + \ldots,$$

where $a_{2n} = O(a_2^n)$, and the ratios a_{2n}/a_{2n-2} are of about the same order of magnitude. From table 5, typical values of a_2, a_4, and a_6 at Southend are 220 cm, 11 cm and 8 cm respectively, so that a_6/a_4 is very much greater than a_4/a_2. This fact, which holds at most shallow water ports, is usually interpreted as being the result of friction enhancing the odd-order harmonics (counting the primary wave as 1st harmonic). But a frictional term of form $ku|u|$ would, in rough terms, be expected to increase a_6 in the order a_2^2, in contradiction to my assumed interaction form $(\tilde{\zeta}_2^1)^3$.

The function $x|x|$ is notoriously awkward to handle analytically. In appendix C, I use its expansion in Hermite polynomials to argue that, for bounded oscillatory variables such as tides, a finite odd order polynomial such as

$$k_1 x + k_3 x^3$$

can be defined which differs from $x|x|$ by negligible amounts. In fact since the frictional coefficient k almost certainly varies with the current strength, there seems to be no compelling reason for adhering strictly to the nonanalytic expression. The polynomial approximation implies that a variation of a_6 proportional to a_2^3 could be fitted to the data reasonably well. It remains to verify whether this is so in the present case.

To this end, values of

$$a'_n = \frac{1}{25} \sum_{r=-25}^{25} (1 + \cos \pi r/25)\, e^{2\pi i r n/25}\, \zeta(t + r\Delta t) \quad (n = 2, 4, 6, 8)$$

were computed at 48 h intervals from the hourly records at Immingham and Southend. Obviously, the a'_n correspond in a realistic way to the a_n, and the variation of $|a'_2|$ from spring

to neap tides provides a limited variation of primary wave amplitude. For the period 21 March to 21 September 1959, which was fairly free from weather disturbances, values of $|a'_4|^2$, $|a'_6|^2$, and $|a'_8|^2$ are plotted against $|a'_2|^2$ on logarithmic scales in figures 4·1, 4·2. The straight lines correspond to power laws of form $|a'_2|^{\frac{1}{2}m}$, regardless of whether the plotted points lie close to the line or not. Various degrees of scatter are present on all diagrams, due to noise and frequency variation, but it is clear that the values of a'_6 fit a cubic law very well at both places. The assumed form of interaction is therefore justified, at least in the present application.

P. Lal of Liverpool University Tidal Institute has shown (unpublished MS.) that at Tilbury, some 15 miles up the river from Southend, a_6 is very slightly closer to the form $(|a_2| + \text{constant})^2$ than to $|a_2|^3$. He justifies the squared expression approximately in terms of quadractic friction. However, the cubic is still the best pure power law which fits the Tilbury data, and one wonders if this is generally true in other shallow water areas.

The results for a'_4 and a'_8 also require some comment. The dependence of the double interaction on frequency, noted earlier, tends to confuse the results for a'_4. At Southend, for example, the harmonic constituents lead us to expect about the same value of a'_4 at spring tides near apogee (M_2 and S_2 in phase, N_2 in antiphase) as at neap tides near perigee (M_2 and N_2 in phase, S_2 in antiphase). However, the total absence of any trend in the first diagram of figure 4·2 is also due to an abnormally high noise level in the species 4 frequency band at Southend. Analysis shows a residual nontidal variance in a bandwidth of 11 c/m centred on species 4, of value 36 cm^2 (noise : signal ratio 61 %), compared with 5 cm^2 in species 3, 1 cm^2 in species 5, and 3 cm^2 in species 6. The nontidal variance in species 4 at Immingham is only about 2 cm^2, so the corresponding diagram in figure 4·1 shows a reasonable trend, though evidently not a simple square law.

The reason for the high species 4 noise at Southend is obscure. It suggests that the double (but not the triple) interaction is unstable at that place, and therefore sensitive to slow changes in such conditions as mean sea level, fresh water run-off, etc. The double interaction is certainly peculiar, in that its phase lead is slightly negative (see figure 3), implying a tendency to steepen the *rear* face of the primary wave, not the forward face as is common in simple cases.† An analysis which allowed for a triple interaction of form $\bar{\zeta}\tilde{\zeta}^{\mathrm{I}}_2\tilde{\zeta}^{\mathrm{I}}_2$, where $\bar{\zeta}$ is the computed local low frequency sea level, attributed about 6 cm^2 to the triple interaction, leaving about 30 cm^2 still unaccounted for.

The diagrams for a'_8 are unimportant, since the fourth harmonic is very weak. Southend well supports a fourth power law, but Immingham hardly. I did not investigate this harmonic any further.

(*c*) *Predictable variances*

Table 5 shows for each tidal species at each port:

(*a*) the 'predictable variance', that is, the reduction in variance when the relevant response prediction is subtracted from the recorded sea level;

(*b*) the predictable variance for a 'harmonic' tidal prediction (see below);

(*c*) the total spectral variance in a bandwidth 9 c/m for species 1, 2, 3, 11 c/m for species 4, 5, 6.

† However, the relation between the phase of the second harmonic and wave steepening is complicated by the presence of a strong third harmonic.

PHILOSOPHICAL TRANSACTIONS OF THE ROYAL SOCIETY A MATHEMATICAL, PHYSICAL & ENGINEERING SCIENCES

The harmonic predictions were included to provide a comparison. The selected constituents used are listed in table 2, and their numerical values taken from standard lists, with one exception based on analysis of a year's data within the current 3 y period. (The exception was Immingham, I.H.B. sheet no. 915, whose constants were derived from 1956–57.)

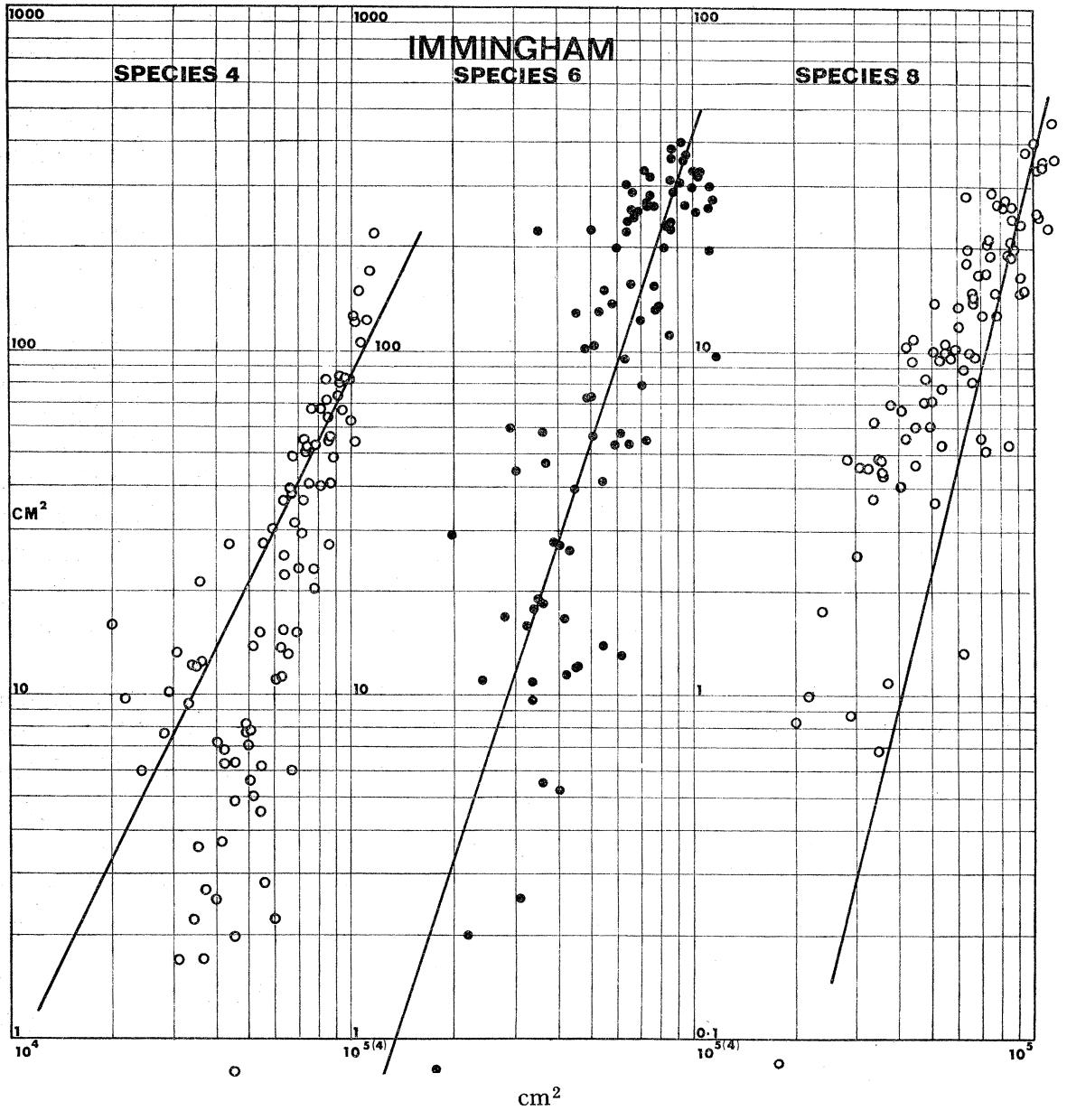

FIGURE 4·1. Squared amplitudes of second, third and fourth harmonics to the semi-diurnal tide at Immingham for the period 21 March to 21 September 1959. The straight lines represent possible second, third and fourth power laws, respectively.

The numbers of constants were chosen to be in no case fewer than the numbers of weights used in the response method. All constituents omitted here were very small in amplitude, the largest being the diurnal constituents 00_1, whose amplitude is about 1·0 cm at Stornoway, Aberdeen, and Southend, and π_1, which has 1·4 cm at Immingham. In general, it is unlikely

that inclusion of a few more constituents than are given in table 2 could increase any predictable variance by more than 1 cm^2.

For the top three ports, all fairly well exposed to the ocean, prediction variances from the two methods are about equal. Only in species 4 does the harmonic prediction with five pairs

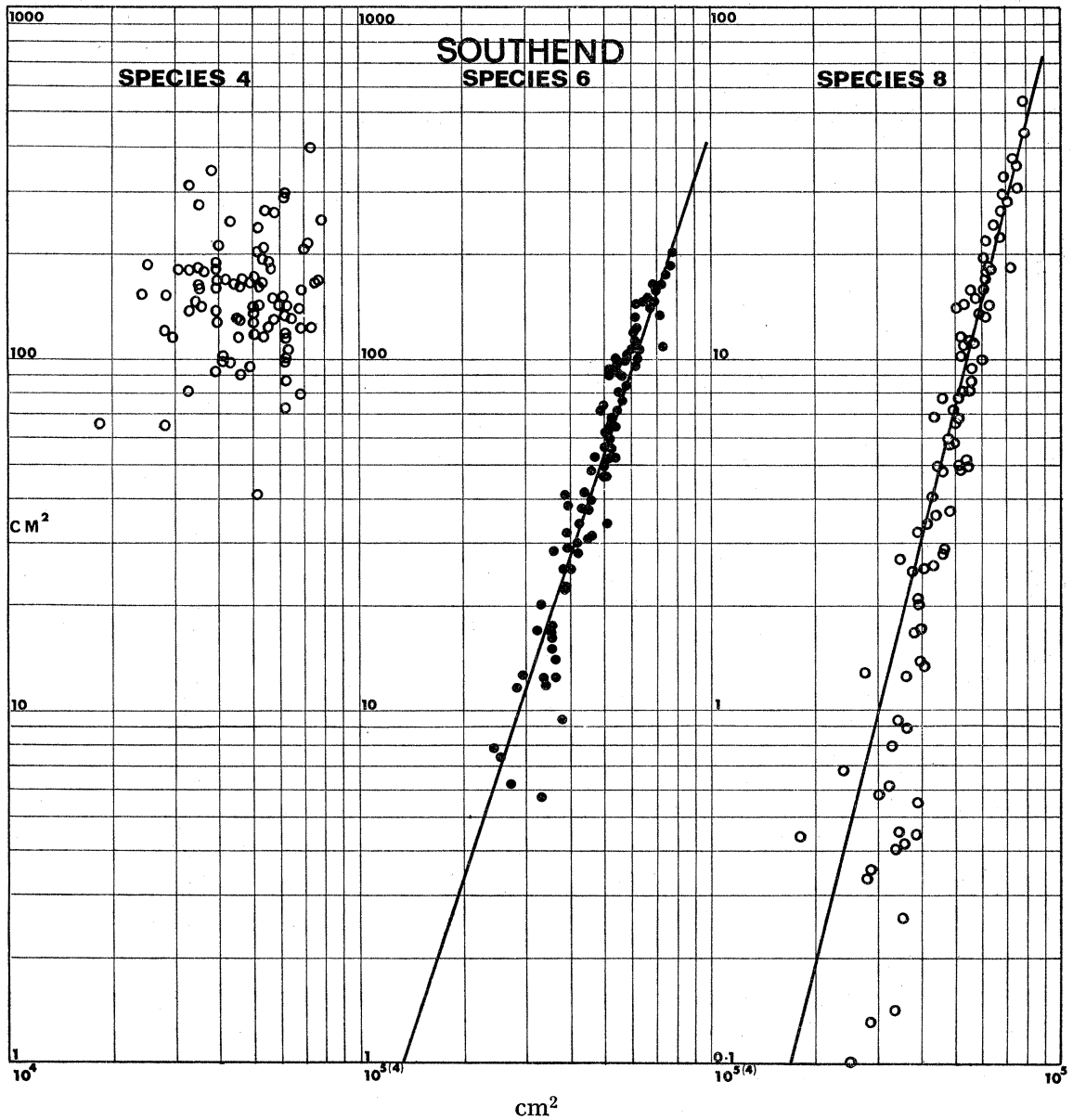

FIGURE 4·2. As figure 4·1, for Southend.

of constants better the response prediction with three pairs, by a small margin. Aberdeen, Immingham, and Southend are progressively affected by the shallow water complex of the North Sea and its estuaries. We see that the response method improves the predictable variance over the harmonic method by increasing amounts. At Southend, the overall improvement is 56 cm^2 (which could be increased to 62 cm^2 if we included the $\overline{\zeta}\,\tilde{\zeta}^{\mathrm{I}}_{2}\tilde{\zeta}^{\mathrm{I}}_{2}$ interaction referred to in the previous section).

The suggestion is therefore that the simple interaction products included in the response method deal more effectively with the shallow water distortions than the assortment of spectral lines, with somewhat dubious modulations, normally used in the harmonic method. Recently, Zetler & Cummings (1967), and Lennon & Rossiter (1967), have greatly extended the normal number of harmonic constituents for certain shallow water ports. In particular, Lennon & Rossiter increased the predictable variance at Southend for the year 1961 by 0·023 ft.^{2} (21 cm^2), by increase of the number of pairs of constants from 60 to 113. Although direct comparison with the present figures is not quite fair, it would appear that the response method produces at least as good an improvement with only 26 pairs of constants.

TABLE 5. PREDICTABLE (*a* AND *b*) AND TOTAL (*c*) VARIANCES (cm^2)

tidal species		1	2	3	4	5	6
Malin Head	*a*	70	7595	6·5	4·1	0·08	0·18
	b	69	7594	6·2	4·3	—	0·16
	c	77	7616	9·1	6·2	0·55	0·59
Stornoway	*a*	113	12478	5·8	46·7	0·02	0·69
	b	113	12478	5·6	47·5	—	0·66
	c	117	12486	8·4	50·9	0·60	1·10
Lerwick	*a*	50	2155	0·3	2·2	0·01	2·23
	b	50	2155	0·3	2·3	—	2·19
	c	52	2157	0·6	2·5	0·14	2·51
Aberdeen	*a*	118	10495	1·5	7·4	0·05	0·51
	b	114	10490	1·1	6·5	—	0·00
	c	130	10513	2·8	9·7	0·54	1·83
Immingham	*a*	216	31175	12·8	12·5	1·12	5·48
	b	209	31148	8·6	12·2	—	4·89
	c	244	31221	15·4	14·3	2·10	7·68
Southend	*a*	127	24613	23·1	58·7	0·71	30·67
	b	125	24575	11·2	57·9	—	28·86
	c	159	24668	28·6	95·2	1·53	33·42

It would be interesting to apply similar comparisons to ports with still stronger non-linearity, where it would probably be necessary to increase the number of constants in the response method, by including higher order interactions. One fourth order interaction, namely $(\tilde{\zeta}_2^1)^4$ with energy around 8 c/d, was included in the present analysis, but it accounted for only 5 cm^2 predictable variance at both Immingham and Southend, and negligible values elsewhere.

The total variances for the species bands, listed in rows '*c*' in table 5, are of course upper bounds for any prediction. It is interesting to note that these totals exceed the predictable variances most where '*a*' most exceeds '*b*', that is, at the shallower ports. The anomalous residue of 36 cm^2 in species 4 at Southend was discussed in the previous section. There is also 'tidally unpredictable' variance in the low frequency end of the spectrum, and between the tidal bands. We shall consider these zones later.

5. SURGE-TIDE INTERACTION (RESULTS)

(*a*) *Analysis of data*

Since the purely tidal interactions are largely accounted for by perturbations of order 2 and 3, we may expect the interaction between nontidal and tidal motions to behave similarly. This applies particularly to the North Sea ports, where tides and surges travel

down the coast of east Britain in close association. In fact Immingham and Southend were the only ports for which any nontidal interaction was detectable by the present methods.

Bispectral analysis as described in § 2 (*d*) was performed with ensemble averages from 36 sets of spectra H_r defined by (2·10) with $N = 236$, $t = 3h$, and t_0 at intervals of $29\frac{1}{2}$ days. The 36 overlapping 59 day stretches of data virtually spanned the whole 3 y period available. All places, except the two just mentioned, gave generally low bicoherences and consequently scattered estimates of biadmittance. At Immingham and Southend, however, bicoherences up to 0·6 were found over the most favourable frequency ranges. Their results are summarized in figures 5·1 and 5·2.

In each of these figures the top diagram plots the estimates of biadmittance $Z(f_1, f_2)$ (real and imaginary) against the surge frequency f_1. The lower diagram shows the logarithm of the total mean spectral energy density of sea level† against frequency ($f = f_1 + f_2$), and the corresponding energy contributed by the interaction. The ratio of the two energies is the bicoherence, so the distance apart of the curves is its logarithm. Where the lower curve is not shown, the analysis was confused either by tides or by the ambiguity discussed in § 2 (*c*). With 36 degrees of freedom, all bicoherences greater than about 0·03 (log separation less than 1·5) are significant. The confidence ranges of the biadmittances vary inversely with the bicoherence. Many plotted points have ranges much larger than the typical value shown, which is calculated for a bicoherence 0·2 (log separation 0·7), but the ensemble of independent points has greater significance than any individual value.

The values at $f_1 = -2$ were derived from a separate analysis of the interaction between harmonics 114 (M_2) and 118 (S_2, etc.) producing energy at harmonic 4 (MSf). Coherences were about 0·1. The positive real values of $Z(2, -2)$ imply a steady tidal 'set-up' of sea level. On multiplying $Z(2, -2)$ by the mean tidal variance, we get 2 cm set-up at Immingham and about 7 cm at Southend. Of the other stations, only Malin Head showed some coherence at these frequencies, with about 2 cm set-up (see also § 9).

There is considerable scatter; evidently many more data than for 3 years would be necessary to define a smooth curve with accuracy. However, the points do suggest definite trends, which in most cases confirm continuity with the tide-tide interactions, indicated by squares. The rather rapid variations confirm those already noted in the narrow tidal band around $f_1 = +2$ (§ 4 (*b*)). In fact the general characteristics of nearly constant phase and increasing amplitude noted for Immingham in figure 2 are well reproduced at $f_1 = +2$ in figure 5·1. The corresponding curves for Southend do not agree so well, and the tidal values near $f_1 = +1$ appear slightly anomalous, although the large imaginary value there is partially supported by the large surge-tide values at surrounding frequencies. A possible partial failure in the tidal analysis here has already been noted in § 4 (*a*) with regard to the linear admittance in species 3.

The curves drawn in the upper parts of figures 5·1 and 5·2 correspond to a 10-term Fourier series as equation (2·15) with $S = 4$, obtained from a least-squares computation with weights $(\gamma^{-2} - 1)^{-2}$, where γ^2 is the bicoherence of any point. The tidal values were included in the computation with appropriate weights derived from other measures of significance. Values of S greater than 4 were also tested, but gave very slight improvement in fit, and a

† Although the frequency resolution is barely less than 1 c/m, the tapering function in equation (2·10) ensures that sidebands from the tides are negligible.

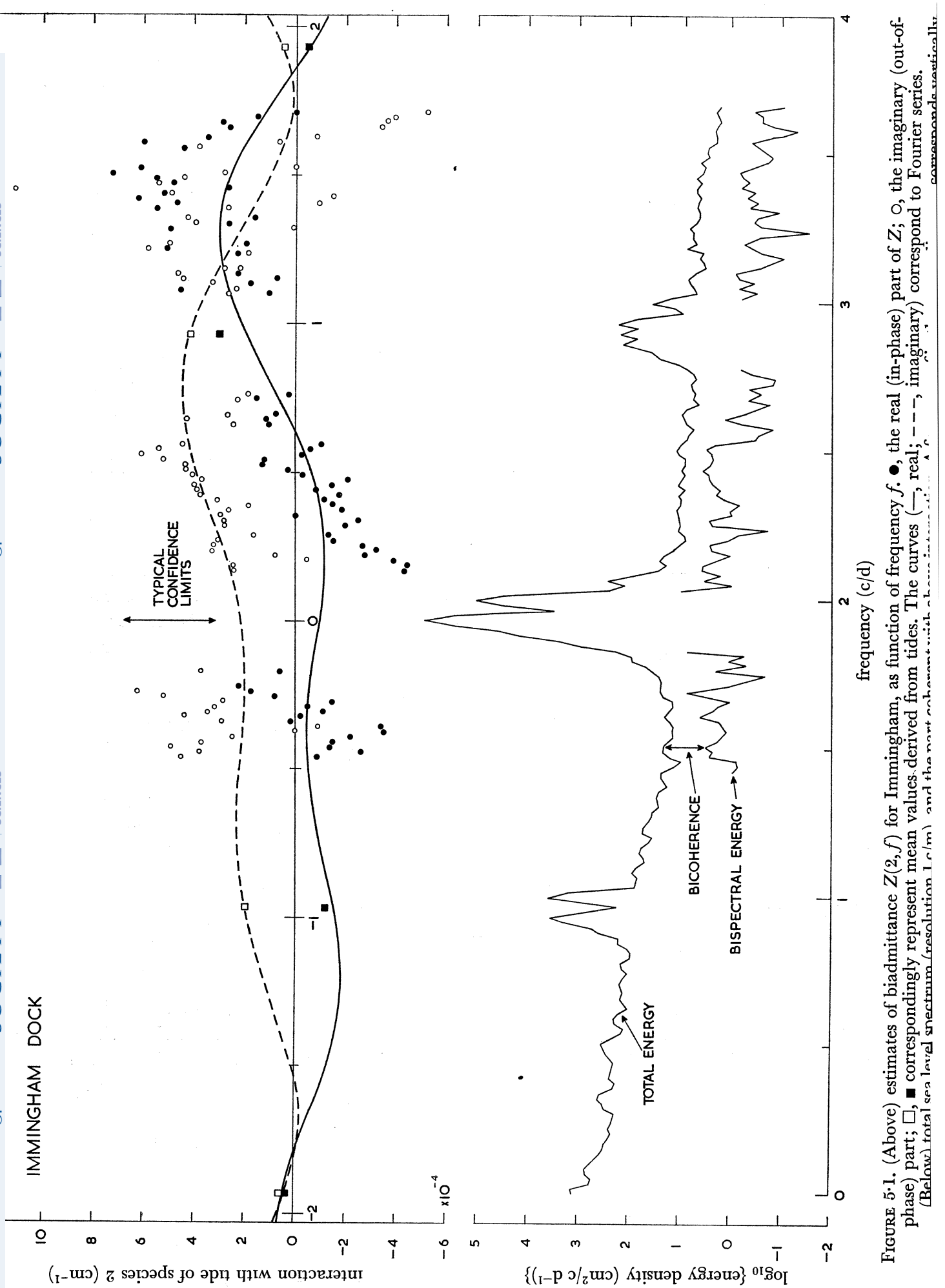

FIGURE 5·1. (Above) estimates of biadmittance $Z(2,f)$ for Immingham, as function of frequency f. ●, the real (in-phase) part of Z; ○, the imaginary (out-of-phase) part; □, ■ correspondingly represent mean values derived from tides. The curves (—, real; – – –, imaginary) correspond to Fourier series. (Below) total sea level spectrum (resolution 1 c/m), and the part coherent with observations [illegible] corresponds vertically

PHILOSOPHICAL TRANSACTIONS OF THE ROYAL SOCIETY A MATHEMATICAL, PHYSICAL & ENGINEERING SCIENCES

PHILOSOPHICAL TRANSACTIONS OF THE ROYAL SOCIETY A MATHEMATICAL, PHYSICAL & ENGINEERING SCIENCES

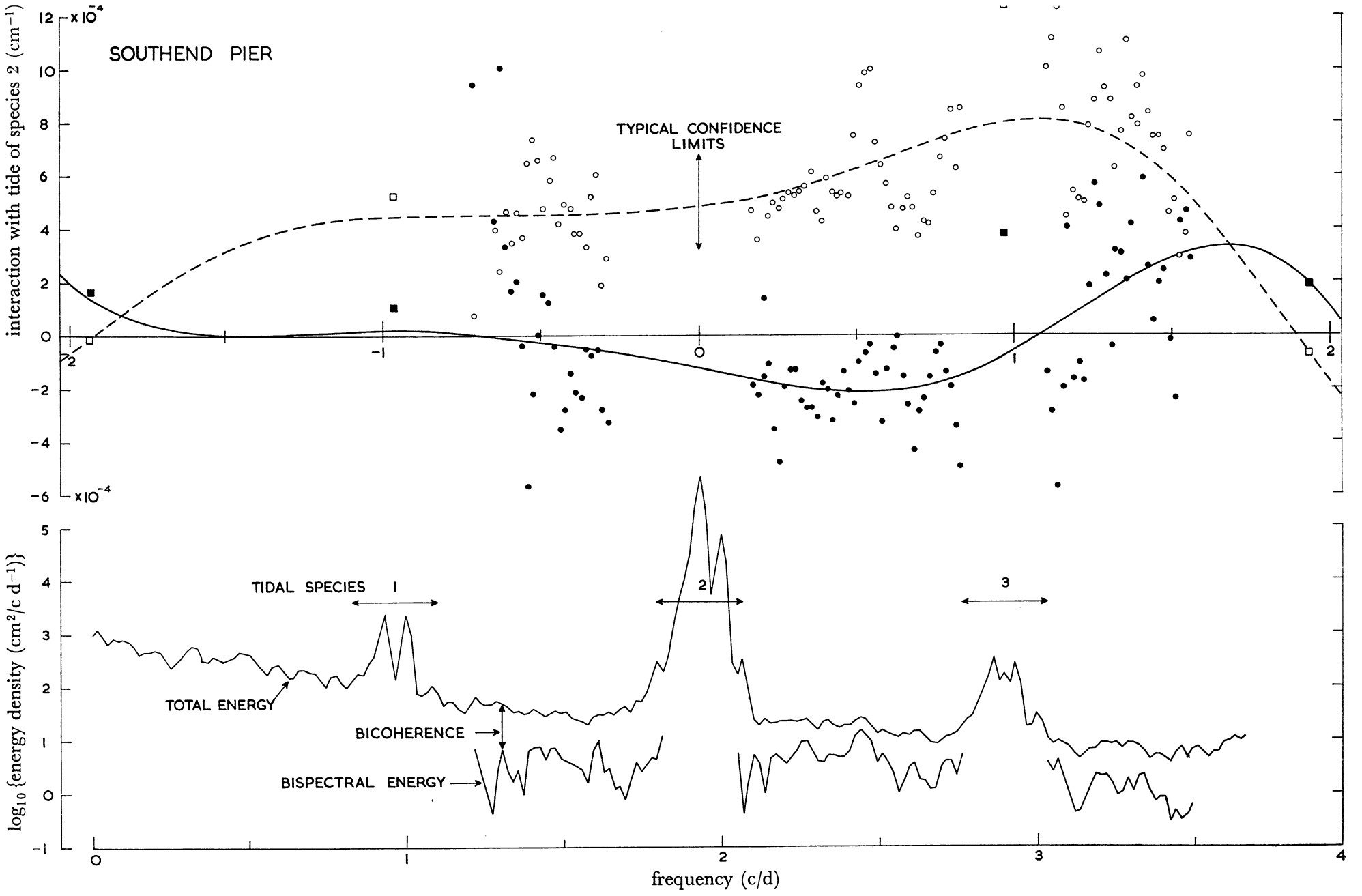

FIGURE 5·2. As figure 5·1, for Southend.

tendency to large coefficients. Further, it seems hardly justified to assign more than 10 arbitrary constants to such scattered data. As pointed out in § 2 (*d*), the coefficients of the Fourier series are applicable to a regression formula for the bilinear interaction (2·16), which could be used for prediction, provided a good linear surge prediction $\tilde{\zeta}_S^1$ is available. The coefficients $R(s, 0)$ for Immingham and Southend are listed in appendix B.

The values of the smoothed curves at $f_1 = 0$ provide a reasonable interpolation between the estimated values near $f_1 = \pm 0{\cdot}5$ c/d for the cusp-forming interaction between tide and mean sea level, first suggested by Munk, Zetler & Groves (1965), and also discussed in M.C. (pp. 570–571). The actual noise energy within the species 2 tidal group will be considered in § 6.

The total bispectral variance, including that derived from other ports of the species 2 tide, amounts to about 4 cm^2 at Immingham and 9 cm^2 at Southend. These variances are quite small, but the interaction will provide a sensible change in the detailed profile of large surges.

The triple surge-tide-tide interaction is divided into two classes, according to whether one takes the sum or difference of the tidal frequencies. With reasoning similar to that given for the bispectral analysis (§ 2 *c*), I investigated $Z(-f_1, 2, 2)$ in terms of the ensemble average

$$\langle (H_{r_1}^* H_{114} H_{114}) H_{r_4}^* \rangle = \langle H_{r_1}^* H_{r_4}^* H_{114}^2 \rangle \quad (r_4 = 228 - r_1), \tag{5·1}$$

114 being the harmonic number which corresponds fairly closely with the M_2 harmonic constituent at 2 c/l.d. In the absence of spectral computations above 3·6 c/d, positive values of f_1 were not attainable (apart from the purely tidal values). Only values of $-f_1$ near $-0{\cdot}5$ c/d gave significant coherences. Since the energy density at $f = 0{\cdot}5$ c/d is very much greater than that at 3·5 c/d, there is no difficulty with ambiguity.

$Z(f_1, 2, -2)$ was derived from the mean product

$$\langle (H_{r_1} H_{118} H_{114}^*) H_{r_4}^* \rangle \quad (r_4 = 4 + r_1), \tag{5·2}$$

118 being the harmonic number corresponding with S_2.† The expected value of this product is (cf. equation 2·13)

$$|H_{118}|^2 |H_{114}|^2 [Z(f_1, 2, -2) |h_1'|^2 + Z(f_4, -2, 2) |h_4'|^2]. \tag{5·3}$$

This is apparently ambiguous, but since for the low frequencies involved,

$$Z(f_4, -2, 2) \doteqdot Z^*(f_1, 2, -2),$$

and the imaginary part of the admittance is approximately zero, (5·3) can be written

$$|H_{118}|^2 |H_{114}|^2 [|H_{r_1}|^2 + |H_{r_4}|^2] X(f_1, 2, -2) \tag{5·4}$$

with fair approximation. In the neighbourhood of $f_1 = 0{\cdot}5$ c/d coherences of order 0·2 were found with this interaction, and (5·4) gave a reasonably consistent set of estimates of $X(0, 2, -2)$.

Table 6 summarizes the triple interaction coefficients from tidal and nontidal analyses. For convenience, the nontidal values are represented by a single average value at the appropriate low frequency. It can be assumed that $Z(-f, 2, -2) = Z^*(+f_1, 2, -2)$.

† Also including K_2, and other lines in the solar group.

PHILOSOPHICAL TRANSACTIONS OF THE ROYAL SOCIETY A MATHEMATICAL, PHYSICAL & ENGINEERING SCIENCES

The individual values vary, but with regard to the wide frequency spacing not more so than the biadmittances plotted in figures 5·1, 5·2. For uniformity with the analysis of biadmittances, the Fourier series with $S = 4$ which fits the values in table 6 exactly were computed, and the coefficients listed in appendix B. Only five coefficients are involved in $Z(f_1, 2, -2)$, because the coefficients of the cosine series which applies to the real part are the same as those of the sine series which applies to the (negative) imaginary part.

TABLE 6. TRIPLE INTERACTION COEFFICIENTS

(Units are 10^{-6} cm^{-2})

		Immingham		Southend	
	f_1	real	imaginary	real	imaginary
$Z(f_1, 2, 2)$	−2	−2·21	−1·60	−6·28	−1·64
	−1	−1·37	−0·16	−2·25	−1·87
	−0·5	−0·63	0·85	−0·88	−0·02
	+1	0·55	−0·90	−1·42	−0·03
	+2	0·16	−0·02	+0·37	−0·46
$Z(f_1, 2, -2)$	0	−0·38	0	−0·53	0
	+1	−1·61	−2·60	−3·05	−3·15
	+2	−2·21	−1·60	−6·28	−1·64

The full regression formulae describing the interactions of order 2 and 3 can now be written

$$\tilde{\zeta}^{\mathrm{II}}_{ST}(t) = \sum_{s=0}^{4} [2\{P_2(s)\,\xi''(t) + Q_2(s)\,\eta''(t)\} + 2\{P_3^+(s)\,\xi^{\mathrm{iv}}(t) + Q_3^+(s)\,\eta^{\mathrm{iv}}(t)\} + P_3^-(s)\,\xi^0(t)]\,\tilde{\zeta}^{\mathrm{I}}_S(t-3s), \tag{5·5}$$

where

$$P_2(s) + \mathrm{i}Q_2(s) = R(s, 0),$$

$$P_3^+(s) + \mathrm{i}Q_3^+(s) = R^+(s, 0, 0),$$

$$P_3^-(s) + 0 = R^-(s, 0, 0),$$

are the pairs of response weights (coefficients of Fourier series) listed in appendix B.

$$\xi''(t) + \mathrm{i}\eta''(t) = \tilde{\zeta}^{\mathrm{I}}_T, \quad \text{the predicted species 2 tide}$$

$$\xi^{\mathrm{iv}}(t) + \mathrm{i}\eta^{\mathrm{iv}}(t) = (\tilde{\zeta}^{\mathrm{I}}_T)^2, \quad \text{a species 4 variable,}$$

and

$$\xi^0(t) = \tilde{\zeta}_T^{I}.\tilde{\zeta}^{\mathrm{I}}_T{}^*, \quad \text{a low frequency variable.}$$

As usual, $\tilde{\zeta}^{\mathrm{I}}_S(t)$ is the primary predicted surge with time in hours.

(*b*) *A model surge*

It is worth demonstrating the action of formula (5·5) in realistic terms, since not only is it unfamiliar, but its coefficients were derived through rather devious processes. To this end, I applied (5·5) to a model surge defined by

$$\tilde{\zeta}^{\mathrm{I}}_S(t) = (1 + \cos 2\pi t/18) \text{ metres} \quad (0 \leqslant t \leqslant 18) \tag{5·6}$$

(zero before and after), in the presence of a simplified 'spring tide'

$$\tilde{\zeta}^{\mathrm{I}}_T(t) = 3\,\mathrm{e}^{-2\pi\mathrm{i}(t-t_0)/12} \text{ metres.} \tag{5·7}$$

In turn t_0 was given the values 9, 6, 3, 0 h, to simulate the cases of the primary surge peak

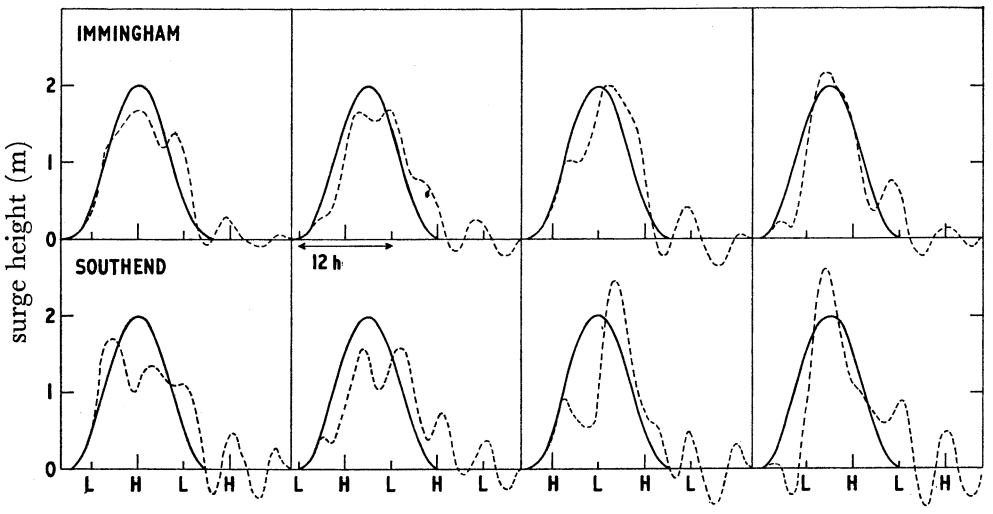

FIGURE 6·1. A hypothetical surge, whose linear part (—) coincides with (from left to right) High, falling, low, and rising tide, at Immingham and Southend. The broken lines represent the effect of adding surge-tide interaction (equation (5·5)). Range of tide 6 m. H and L denote tidally predicted times of High and Low Water.

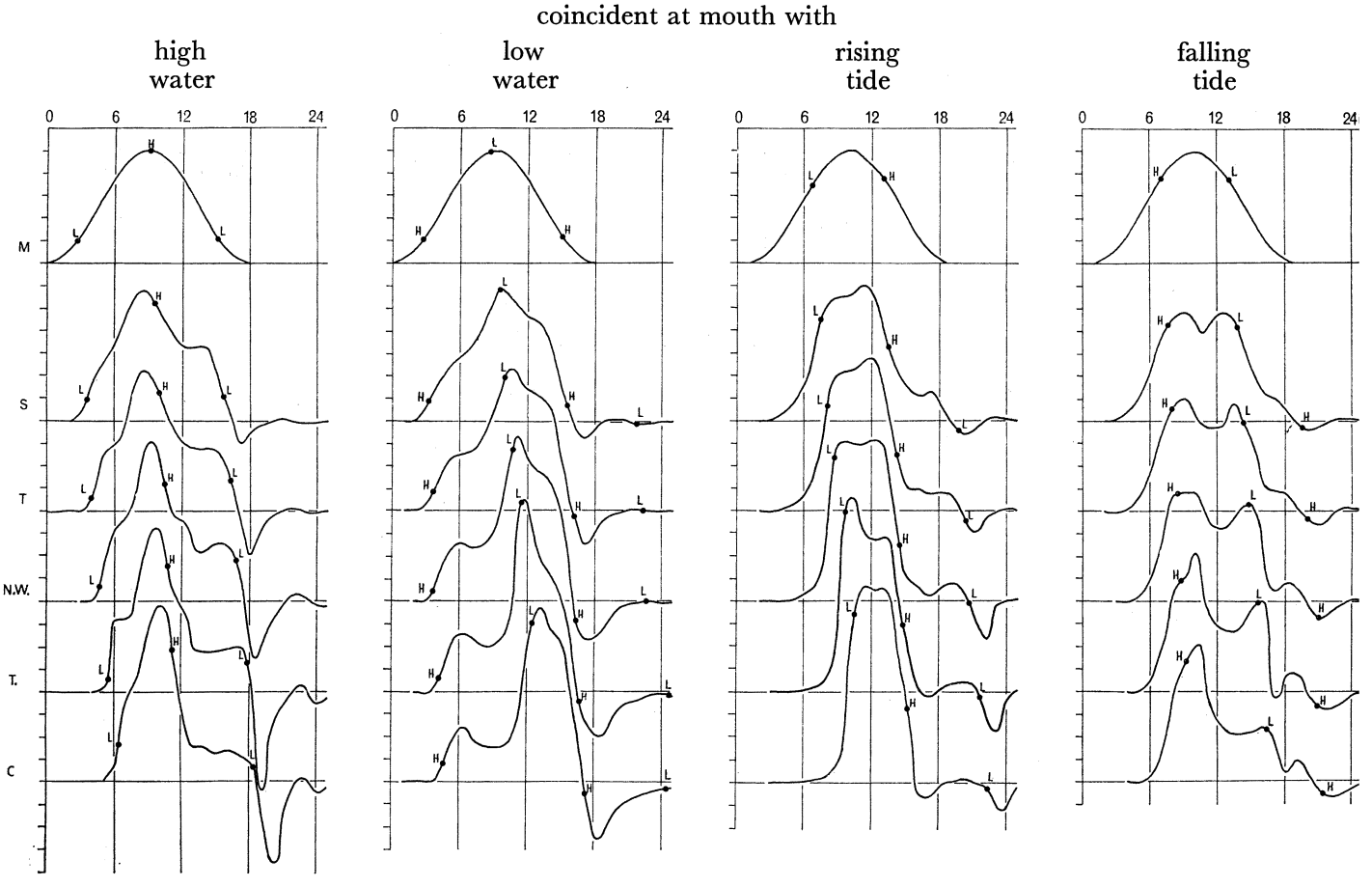

FIGURE 6·2. Calculated profiles (by G. W. Lennon) of a surge propagating up the River Thames, (Mouth, Southend, Tilbury, N. Woolwich, Tower Pier, Chelsea Bridge). Initial profile similar to linear surge in figure 6·1. Range of tide 20 ft. H and L have same meaning as in 6·1, but order of diagrams from left to right is different.

PHILOSOPHICAL TRANSACTIONS OF THE ROYAL SOCIETY A MATHEMATICAL, PHYSICAL & ENGINEERING SCIENCES

($t = 9$) coinciding with high, falling, low and rising tide respectively. All dimensions are typical of large surges and tides occurring at both Immingham and Southend.

The results for $\tilde{\zeta}^{\mathrm{I}}_{S}$ and $\tilde{\zeta}^{\mathrm{I}}_{S}+\tilde{\zeta}^{\mathrm{II}}_{ST}$ are sketched in figure 6·1, where the relative phase of the semi-diurnal tide is indicated by the times of predicted high and low water. The effects of the interaction are rather similar at the two places, but more pronounced at Southend, as expected. In general terms, they confirm the effects noted by Rossiter (1961) and others, that surges tend to be reduced at high and falling tide but increased when their peaks coincide with low or rising tide. The importance of the triple interaction term, producing oscillations of roughly 4 c/d, is evident.

In detail, the curves are remarkably similar to some unpublished results† of G. W. Lennon from computations of nonlinear wave propagation in the Thames Estuary, reproduced in figure 6·2. In Lennon's computation, a cosine wave of 5 ft. amplitude similar to equation (5·6) and a tide of 10 ft. range were inserted at a position taken as the mouth of the estuary, and their subsequent progress computed from the quasi one-dimensional differential equations with quadratic friction. Conditions are not precisely as in my example, because the 'primary surge' at upstream positions is not defined, but it probably does not differ greatly from the cosine form at the mouth, perhaps with some magnification. The general shapes of the curves at the four states of the tide in figure 6·2 (presented in a different order from figure 6·1) are all similar to each other and to the corresponding curves in figure 6·1. However, my curves from Southend agree best with the curves in figure 6·2 for North Woolwich, about 25 miles up-river. This may be due to Lennon's inevitable choice of an undistorted shape of the surge at the 'mouth' of the estuary, where in actuality some effects of interaction would already be present. On the other hand, Lennon's calculations automatically include the interaction of the surge with itself, which I have perforce ignored.

6. Noise close to tidal frequencies

The analyses of Munk *et al.* (1965) and of M.C. showed a rise in noise level within the principal tidal groups with the appearance of 'cusps' centred on the strong tidal lines. The similarity between the shape of these cusps and the spectrum of sea level near zero frequency suggested that they may represent the interaction between the tide and local mean sea level, but careful investigations in M.C. failed to confirm this hypothesis. Since we have now (§ 5 *a*) established this type of interaction for low frequencies greater than about 0·2 c/d at two ports, it is interesting to see if it still applies in the true 'cusp region', within 1 c/m of the M_2 line.

To do this, we need much finer resolution in frequency than used in § 5 *a*. I therefore computed the simple Fourier coefficients

$$H'_r = \frac{2}{N}\sum_{n=-\frac{1}{2}N}^{\frac{1}{2}N}\{\zeta(n\Delta\tau)-\tilde{\zeta}_T(n\Delta\tau)\}\,\mathrm{e}^{2\pi irn/N} \quad (\Delta\tau = 3h,\ N = 8744,\ 2012 \leqslant r \leqslant 2212) \qquad (6\cdot1)$$

of the full 3 y series of observed (low-passed) sea level ζ less the tidal prediction $\tilde{\zeta}_T$ from the response weights described in § 4, for a series of frequencies spanning the range

$$(2\ \mathrm{c/l.d.} \pm 2{\cdot}5\ \mathrm{c/m}).$$

† Advisory Committee on Oceanographic and Meteorological Research, Ministry of Agriculture, Fish and Food, London, Paper 23vii (October 1965), figure 4.

The resolution is $\frac{1}{3}$ c/y, and the basic period of 1093 days makes negligible sideband effects from unremoved tidal lines at frequencies which are multiples of 1 c/d, c/m, and c/y.

Figure 7 shows the energy density from (6·1) on a log scale for all six stations (upper diagram of each pair). The positions of major tidal frequencies (vertical lines), are in many cases occupied either by a pronounced dip, due to slightly over-effective removal by analysis of the same data, or by a peak, due to incomplete removal. The spectra themselves are jagged because there is no ensemble averaging, which could only be achieved at the cost of lower resolution or more extensive data. Even so, they clearly differ from the c/y resolution spectra presented in M.C., in showing no general tendency (except for Malin) to rise towards the major tidal frequencies. However, the steps at the edges of the diagrams show that the general level is everywhere 3 to 10 times that in the inter-tidal noise regions, 0·5 c/d distant. The general noise level is lowest at Lerwick, where the tides are smallest, and highest at the two estuary ports.

The Λ-shaped humps centred on $M_2(2\,0\,0)$† and $S_2(2\,2\,-2)$ in the diagram for Malin Head were at first very puzzling, especially as there is no sign of such a feature at Stornoway, only 180 miles distant. Their cause was later traced to a slowly accumulating blockage in the gauge's inlet pipe. This produced an artificial phase lag, which built up steadily from mid 1959 to mid 1960, reaching a maximum anomaly of 7° (about $\frac{1}{4}$ h), until the pipe was replaced, when phases returned to a steady level.

The lower of each pair of diagrams is an approximation to the noise spectrum which would result from a pure interaction of the tide with local mean sea level. The plotted values are in fact

$$\sum_r (|Z_0 H_r H_s|^2 + |Z_0 H_r H_s^*|^2)$$

where H_r are the major *tidal* harmonics of $\zeta(t)$ at $r = 2072$ (N_2), 2122 (M_2), and 2186 (S_2), H_s are the low frequency harmonics $1 \leqslant s \leqslant 90$, and the left hand quantity is added at harmonic number $(r+s)$ and the right-hand at $(r-s)$. For the top four places, the interaction coefficient Z_0 was given a hypothetical value of 10^{-4} cm^{-1}; for Immingham and Southend the interpolated values of $Z(0, 2)$ from the bispectral analysis (§ 5) were used.

Comparison of the six pairs shows that:

(i) at Immingham and Southend, where Z_0 has a realistic value, the actual noise level is at least an order of magnitude greater than that of the specified interaction

(ii) with the possible exception of Southend, there is nowhere an obvious correlation of detail between actual and interaction spectra, apart from the seasonal peaks at $(2\,0 \pm 1)$.

Thus, the 'tidal noise level' is again found to be independent of and much stronger than the interaction with mean sea level. More rigorous tests confirmed this result, and also failed to reveal any coherence between the noise spectra at pairs of stations. However, some positive facts did emerge.

If we assume the noise on both sides of (2 0 0) to be due to interaction with or modulation by some (unspecified) low frequency variable with a spectral sequence, F_r say, then the resulting noise contains $H'_{2-r} = \mu_0^* H_2 F_r^*$ and $H'_{2+r} = \mu_0^* H_2 F_r$ (6·2, 6·3)

at the denoted frequencies, where H_2 is the M_2 harmonic, and μ_0 is the interaction coefficient.

† As in M.C., the symbol (IJK) represents a tidal line at frequency $(I$ c/l.d. $+ J$ c/m $+ K$ c/y).

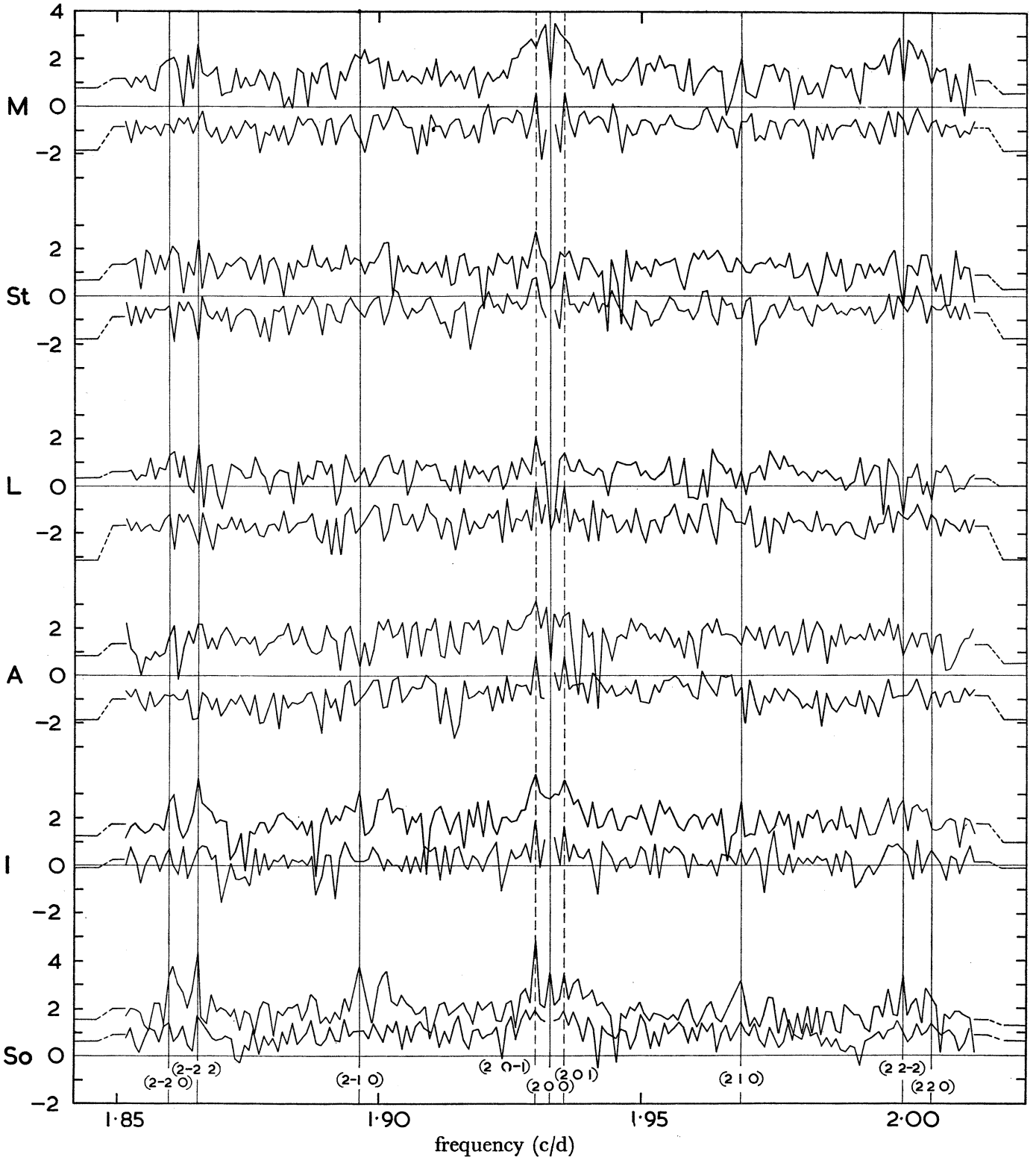

FIGURE 7. For each port, denoted by initial letter, the upper diagram shows the spectrum of sea level inside the species 2 tidal band after subtracting tidal prediction. The lower of each pair shows the spectrum from a hypothetical interaction between tide and low frequency sea level. The stepped horizontal lines at ends of all diagrams show the change in general spectral level after intervals of 0·5 c/d. The vertical lines show the positions of relevant tidal lines.

If μ_0 is purely real, it represents an 'amplitude modulation', and if purely imaginary, a 'phase modulation', while a general complex number represents a combination of the two sorts of modulation. Now the spectra of the *heterodyned* signals corresponding to (6·2) and (6·3) are†

$$H_r''^- = H_2 H_{2-r}'^* = \mu_0 (H_2 H_2^*) F_r \tag{6·4}$$

and

$$H_r''^+ = H_2^* H_{2+r}' = \mu_0^* (H_2 H_2^*) F_r. \tag{6·5}$$

Therefore, allowing for purely incoherent background noise, we may in general expect $H_r''^-$ and $H_r''^+$ to be fairly coherent, and the ensemble average

$$\langle H_r''^- (H_r''^+)^* \rangle \tag{6·6}$$

to have twice the angular argument of μ_0.

I tested the above hypothesis for all six ports, and also for the simultaneous record from Newlyn, using the ensemble average (6·6) over $5 \leqslant r \leqslant 29$ (avoiding the seasonal effect at $r = 3$ and other possible sidebands). The results, listed in table 7 confirm its validity.

TABLE 7. RESULTS FROM HETERODYNING

station	coherence $H_r''^+ : H_r''^-$	double phase 2 arg (μ_0)
Malin	0·365	−85°
Stornoway	0·412	−102°
Lerwick	0·204	−59°
Aberdeen	0·333	−58°
Immingham	0·512	−83°
Southend	0·442	−33°
Newlyn	0·585	−102°

One sees from the coherences that about 40 % of the noise energy (on average) is accounted for by such a mechanism, and that the modulation argument $\theta = \arg \mu_0$ is always well inside one of the quadrants

$$-\tfrac{1}{2}\pi \leqslant \theta \leqslant 0 \quad \text{or} \quad \tfrac{1}{2}\pi \leqslant \theta \leqslant \pi.$$

Thus, both phase- and amplitude-modulations operate. However, the physical identity of the modulating variable remains unknown. Similar tests applied to Honolulu and other Pacific stations failed to show any coherence, so that the process may be confined to the north west European shelf seas, if not the North Atlantic ocean. But the lack of coherence between stations suggests very localized or even instrumental effects are dominant. A test for coherence with the low frequency spectrum of currents through the Dover Strait, as measured by voltages induced in a cable (Bowden 1956), gave almost insignificant results.

The peaks in the residual spectra at $(2\,0 \pm 1)$, causing an annual modulation, deserve special consideration. The higher resolution in frequency enables them to stand out from the rest of the noise better than in the diagrams of M.C., where they were contaminated by sidebands of the central tidal line. The annual modulation already present in the lunar gravity potential‡ has of course been removed with $\tilde{\zeta}_T$, and is in any case distinct in depending on the influence of *solar parallax* on the Moon's orbit, while the residual seasonal

† I am indebted to Walter H. Munk for the idea of 'heterodyning'.

‡ The modulation of the potential is largely due to the 'annual equation' in the Moon's longitude, which was inadvertently omitted from equation (A 18) p. 577 of M.C., but has since been included to sufficient accuracy by addition of a term $-3me_\odot \sin(h_\odot - p_\odot)$.

effect appearing in figure 7 depends presumably on *solar declination*. The two effects have comparable magnitudes. As we have already seen, the peaks are much too large to be accounted for by interaction with local mean sea level (in this case the seasonal variation *Sa*), and it could not conceivably be attributed to interaction between any other tidal lines.

The first column of table 8 shows the double phase angle analogous to the quantity $2 \arg \mu_0$ listed in table 7, but evaluated purely from the peaks at $(2\,0 \pm 1)$. Without the possibility of ensemble averages, there are no estimates of coherence, but the signal:noise ratio is obviously fairly high. No results are given for Malin Head, because the seasonal effect is masked by the hump due to gauge errors, mentioned previously. The results differ significantly from those in table 7 and from each other. There is possibly some geographical relationship, with Stornoway, Lerwick and Aberdeen forming one group, Immingham and Southend another, and Newlyn on its own. Seasonal variations in temperature and rainfall may well affect the estuary ports differently from the others, and perhaps account for the difference between the first and second groups mentioned.

TABLE 8. SEASONAL MODULATIONS

place	double phase	100δ	ϵ	α	β
Malin	—	—	—	—	—
Stornoway	−110°	0·40	0·30°	293°	77°
Lerwick	−106°	0·40	0·30°	242°	40°
Aberdeen	−70°	1·25	0·51°	245°	56°
Immingham	−181°	0·35	1·32°	335°	60°
Southend	−187°	0·83	1·43°	011°	75°
Newlyn	−264°	0·91	0·57°	329°	286°

The remaining four columns of table 8 express the total seasonal modulation to the (2 0 0) tide in the approximate form

$$[1+\delta \cos(\sigma t+\alpha)]\, H_2 \exp[i\omega t + i\epsilon \cos(\sigma t+\beta)], \qquad (6{\cdot}7)$$

where $H_2 e^{i\omega t}$ is the undisturbed tide, δ and α are parameters of amplitude modulation, and ϵ and β of phase modulation. The arguments $\sigma t+\alpha$, $\sigma t+\beta$ increase with the Sun's mean longitude, zero at the Vernal Equinox (about 21 March). The same geographical distinctions apply as in the first column, with some anomalies. Generally speaking, the parameters δ and ϵ have comparable magnitudes, though the larger phase modulations at the estuary ports are perhaps significant. Amplitude modulations tend to be maximum about the months March to June, and phase modulations (which except for Newlyn are remarkably consistent) in January to February.

Corkan (1934) made a fairly extensive study of annual modulations to M_2, including some estimates from four ports included in the present paper, and some from other oceans. His results are difficult to compare with the present ones because he is concerned with the *total* measured constituents at $(2\,0 \pm 1)$, including the part due to the annual equation in the potential, to which I referred earlier. Some of his values estimated from only one year's data must be contaminated by noise. With these reservations, Corkan's findings that greatest tidal ranges tend to occur about June (his α, being based on 1 January, is about 80° less than my α), and that the constituent of lower frequency tends to have greater amplitude than the other, are in general agreement with my results. Corkan was unable to offer a

PHILOSOPHICAL TRANSACTIONS OF THE ROYAL SOCIETY A MATHEMATICAL, PHYSICAL & ENGINEERING SCIENCES

definitive explanation of the cause of the phenomenon, and apparently no further light has been shed on the problem in the 33 years since his paper was written.

Many seasonally varying oceanic quantities, such as currents, depths, ice boundaries, densities, could have an influence on the tides, and it would be very difficult to identify which is the most important. As with the seasonal variation of sea level itself, the effect could be accommodated in the 'response tidal analysis' empirically, through the product $c_2^2\chi_1^0$.

To summarize my findings on tidal modulations, there are three distinct spectral zones:

(i) relatively high frequency modulations of some cycles per month, which at shallow water ports can be attributed to interaction with the local low frequency sea level,

(ii) a zone of higher energy level, recognizable within 1 c/m of M_2, with coherence between left- and right-hand sides, but whose parent low frequency variable is undiagnosed,

(iii) the annual modulations, of still greater energy density (though only a few square centimetres total energy), with phase characteristics again distinct from (ii).

7. Response to weather

(*a*) *The pressure coefficients*

The method used in this paper to define the external forces due to air pressure and wind, and to evaluate the response of the sea surface to these forces has been outlined in §§ 2 (*b*), 2 (*c*) and 3. In brief, the weather forces were represented by a six-component time series $\{p_{00}(t)\ldots p_{02}(t)\}$, being the coefficients of a Taylor expansion (2·8) in x (east) and y (north). Each set of coefficients was evaluated from pressure $P_1(t)\ldots P_8(t)$, recorded at eight stations to fit (2·8) in a least squares sense, so that

$$\{p_{00}(t)\ldots p_{02}(t)\} = \{M\}\{P_1(t)\ldots P_8(t)\}',$$

where M is a constant 6×8 matrix depending only on the distance coordinates of the stations. Sea levels were correlated with the sixfold time series over the spectral range $0 \leqslant f \leqslant 3{\cdot}6$ c/d, equation (2·11) being used to distinguish partial from total coherences. Frequencies in the tidal bands were avoided in all subsequent analysis, because in the present context the tides are virtually 'noise' of very high energy, including even some spurious correlation with the atmospheric tide.

Table 9. Total correlation ratios between pressure coefficients $p_{mn}(t)$

suffixes	00	10	01	20	11	02
00	1	−0·136	0·200	−0·397	0·147	−0·570
10	—	1	−0·047	0·024	0·262	0·061
01	—	—	1	−0·098	−0·098	−0·140
20	—	—	—	1	0·183	0·470
11	—	—	—	—	1	0·104
02	—	—	—	—	—	1

Some of the correlation ratios between the 8744 sets of $p_{mn}(t)$, listed in table 9, are substantial. In general terms, one expects small correlations between pairs such as (00, 10) and (10, 20), because, for example

$$p\frac{\partial p}{\partial x} = \frac{1}{2}\frac{\partial}{\partial x}(p^2)$$

and there is little tendency for the variance of pressure to increase towards east or west. Similarly, one expects large correlations at (00, 20), (00, 02) and (20, 02) because, for example

$$p\frac{\partial^2 p}{\partial x^2} = -\left(\frac{\partial p}{\partial x}\right)^2 + \frac{\partial}{\partial x}\left(p\frac{\partial p}{\partial x}\right)$$

has an obvious tendency to be negative. The relatively large values at (00, 01) and (10, 11) are due to the tendency of the largest extremes of pressure such as centres of depressions to pass over the northern part of the area. Evidently, one would get misleading results by treating any one of the six variables as an independent exciting force. On the other hand, the partial admittances obtained by solving (2·11) are in a real sense independent.

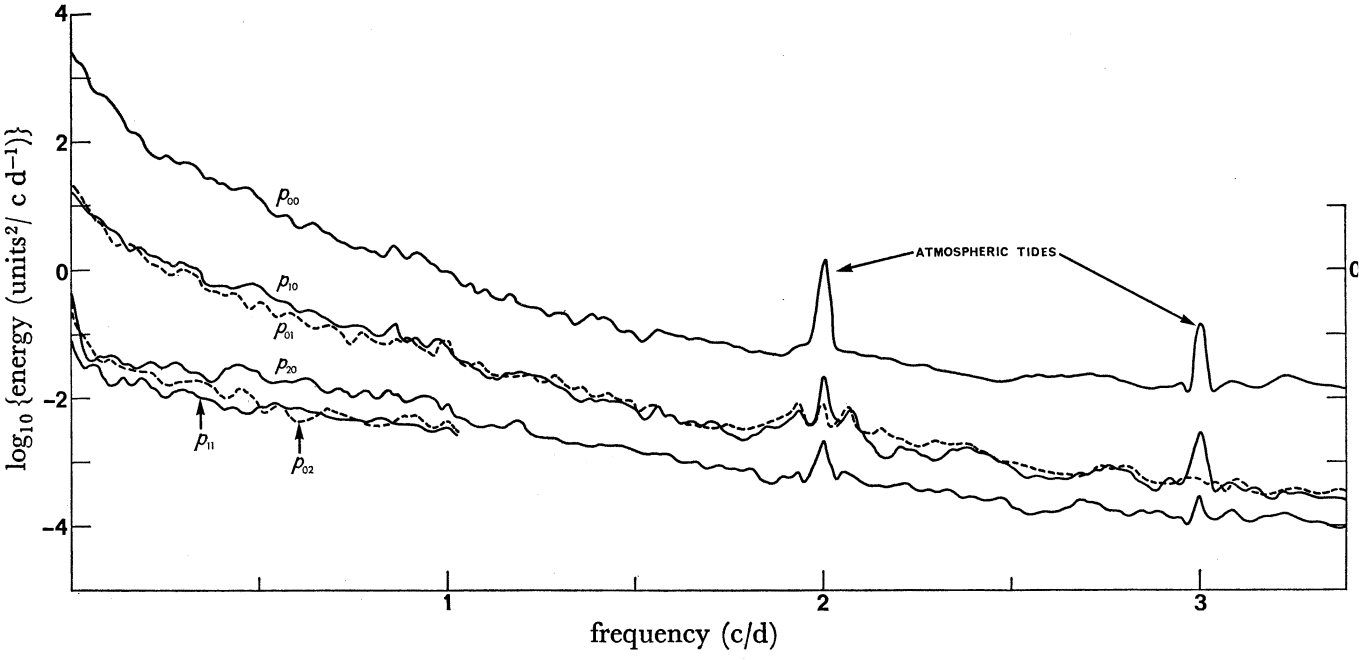

FIGURE 8. Energy spectra of atmospheric pressure coefficients (resolution 1 c/m). Spectra of p_{01} and p_{02} are broken for clarity. Units are millibars and degrees.

The energy spectra of the pressure coefficients are drawn in figure 8. They all share a monotonic descent with increasing frequency, common to many geophysical quantities. Spectra for p_{11} and p_{02} are not shown above 1 c/d, because they are both qualitatively similar to that for p_{20}. The atmospheric tides at 2 and 3 c/d stand out clearly above the background noise, but the diurnal tide is swamped in every case, as commonly observed at these latitudes. In general, the energy at frequencies greater than 1 c/d is less than 0·1 % of that below 1 c/d, so sensible contributions to sea level can be expected only from the low frequency region.

Figure 9 shows a set of partial admittances (solutions of (2·11)) of the sea level at Aberdeen to the six pressure coefficients, at frequencies below the diurnal tides. Values above 1 c/d are too scattered to show any coherent pattern. Definite trends are clearly visible within the range shown, and again one finds considerable variation with frequency. Some of the variation is no doubt due to the distance of some 150 miles between Aberdeen and the origin of the Taylor expansion (2·8). But I have made other, less sophisticated,

comparisons between sea level at some of the present stations and *local* barometric pressure and gradients (for example, figure 2 of Tucker, 1963) and found qualitatively similar variations with frequency.

In particular, one sees that the admittance to the 'spatially constant pressure' p_{00} is near the static value of −1 cm/mb at frequencies below 0·25 c/d, but departs from the static response at higher frequencies. Departures from static response round the Australian coast have been

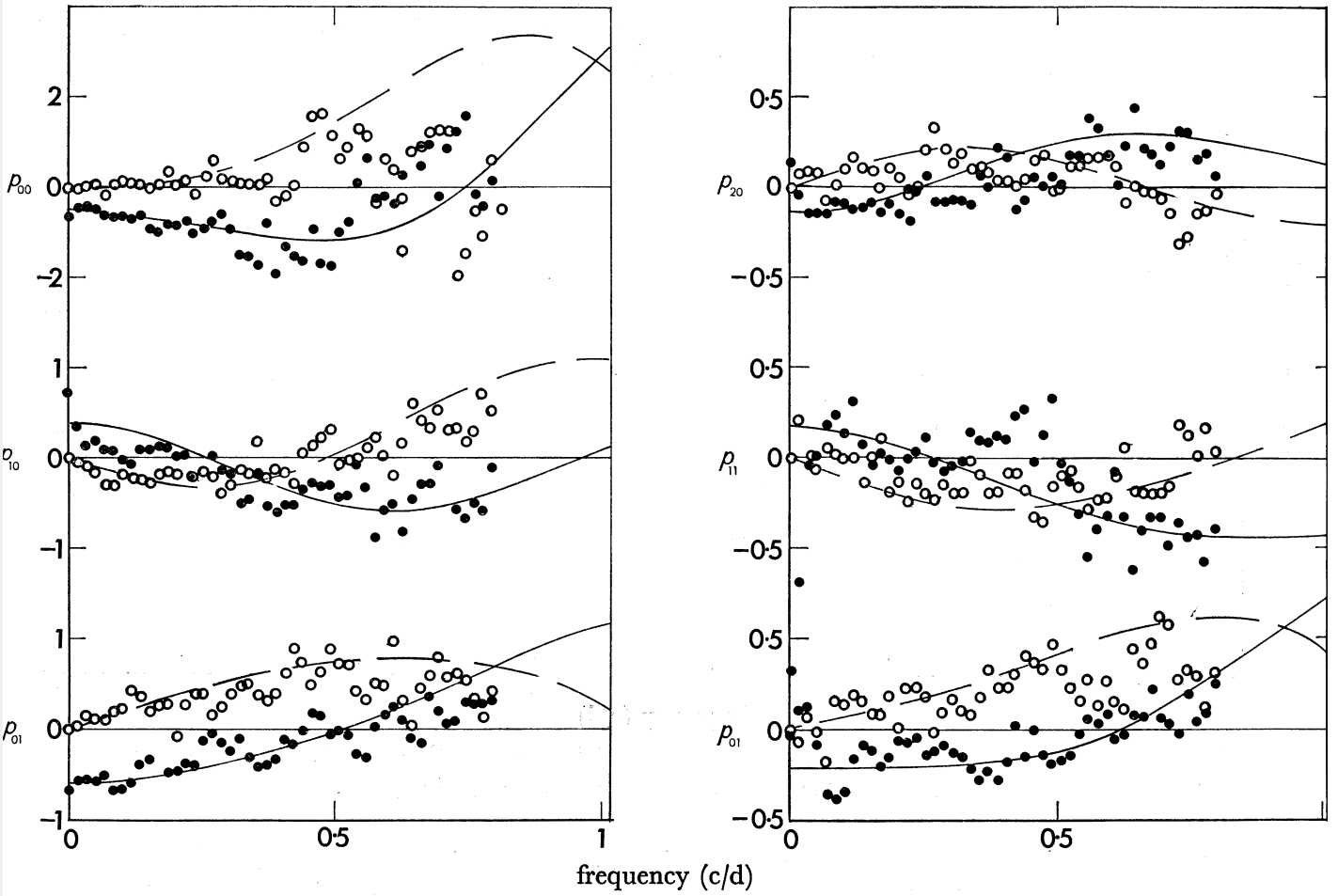

FIGURE 9. Partial admittances of Aberdeen sea level to pressure coefficients. Full circles and lines—real (in phase); open circles and broken lines—imaginary (out of phase). The lines are calculated Fourier series, based partly on values at higher frequencies. Units: p_{00}, cm/mb; p_{10} and p_{01}, cm/mb 10°; p_{20}, p_{11}, and p_{02}, cm/mb $(10°)^2$.

studied by Hamon (1966 and earlier papers). It appears to be a feature to be expected on continental shelves, due to wave-trapping and other forms of resonance (Robinson 1964). E. T. Buchwald (private communication) has developed a theory whereby wind stress plays a major role in generating long waves on shelves, and which may account for an apparent dynamic response to normal pressure through the small correlation between pressure and its gradients (cf. table 9). The present analysis should eliminate such oblique relationships, but the complicated shape of the British shelf and the generally more rapid movement of pressure systems may allow other dynamic effects. On the other hand, Munk

& Bullard (1963) have shown that the response to normal pressure is virtually static, at least up to 1 c/d, at Honolulu (oceanic island) and La Jolla (coast with very narrow shelf), and Hamon (1966) finds a similar result at Lord Howe Island (oceanic).

With multiple correlated input functions as here, partial coherences are complicated to define or interpret. As a realistic measure of the relative effectiveness of the weather variables, the first four rows of table 10 give the total variance of sea level at Aberdeen in various inter-tidal frequency bands, and the residual variances when various groups are included in the prediction. (The residual variances are 'total less predictable', predictable variance being as usual the product of the right and left column vectors of (2·11), summed over the appropriate spectral range.) We see that the variances are reduced by nontrivial amounts relative to the original value in each band as the constant pressure, the first derivatives, and the second derivatives, are successively included. All variables are therefore relevant to the response formalism. Results for other stations are similar.

By subtraction, we find that the weather variables supply a total of 158 cm^2 predictable variance, of which the constant pressure p_{00} contributes 96 cm^2. It is not possible to estimate how much of the contribution of the pressure gradients is due to the wind which is roughly proportional to them, and how much to their improvement in defining the field of normal pressure.

TABLE 10. RESIDUAL VARIANCES (cm^2) OF ABERDEEN SEA LEVEL WITH WEATHER AND 'EXTERNAL SURGE' VARIABLES (S = STORNAWAY ETC.)

	frequency band (c/d)			
variables included	0 to 0·5	0·5 to 0·8	1·1 to 1·8	2·1 to 2·8
none	181	16	9·6	4·1
p_{00}	88	13	9·1	3·9
$p_{00}p_{10}p_{01}$	49	9	7·1	3·6
$p_{00}p_{10}\cdots p_{02}$	38	6	5·3	3·3
ditto + S	21	4	5·0	3·2
ditto + $S+L$	14	3	4·2	3·0
ditto + $S+L+M$	13	3	4·0	2·9

The response (prediction) formula

$$\tilde{\zeta}_s(t) = \sum_k \sum_{m=0}^{M} P_m^{(k)} p_k(t-m\Delta\tau) \qquad (7\cdot1)$$

was derived, as discussed in § 2 (*c*), by Fourier series analysis of the admittance estimates $Z_n(f)$ over the whole frequency range 0 to 3·5 c/d, with least-square weights equal to predictable variance. Thus, taking p_{00} as an example, the expression

$$\sum_r W_r[(P_0+P_1\cos\theta_r+P_2\cos 2\theta_r+\ldots+P_M\cos M\theta_r-X_r)^2 + (-P_1\sin\theta_r-P_2\sin 2\theta_r-\ldots-P_M\sin M\theta_r-Y_r)^2] \qquad (7\cdot2)$$

was minimized, where $\theta_r = 2\pi f\Delta\tau$, f being the frequency corresponding to the spectral sequence r, and

$$W_r = (X^2+Y^2)\,G_r,$$

G_r being the energy spectrum of p_{00}. $\Delta\tau$ was taken as 3 h in all cases, to permit arbitrary variations of admittance within a range of 4 c/d.

A total of five terms ($M = 4$) gave admittance curves which were obviously too smooth to model the variations of the estimated values (X_r, Y_r), showing that the responses require time lags greatly in excess of 12 h. This accords with recent (unpublished) studies of the response of the North Sea to step-function disturbances by Ishiguro and others, although many early investigators attempted to fit regression formula with much smaller, or no time lags. Finally, time lags up to 24 h ($M = 8$) were chosen, as giving reasonable results, allowing for the scatter of the data (figure 9) and the heavier weighting at low frequencies. The complete weather response, using all six pressure coefficients, thus embody 54 (real) weights $P_m^{(k)}$. Note that $m = 0$ is necessarily used for completeness. This implies that, for practical prediction of sea level in real time, the weather itself is assumed predictable at least 3 h ahead.

It should be added that in minimizing (7·2) it was found necessary to omit the value of r at and below the seasonal frequency of 1 c/y in both sea level and the atmosphere, because the anomalous relationship there due to thermal effects often seriously biassed the curve-fitting. The prediction formulae therefore give an anomalous contribution to sea level at very low frequencies. Such anomalies can be absorbed by self-prediction (§ 8).

Little can be learnt from the numerical values of the weights $P_m^{(k)}$ themselves. A typical set, corresponding to the smoothed admittance curves for Aberdeen (figure 9), is given in table 11. As with the tidal weights, it seems to be difficult to obtain by these methods a set of numbers which are smooth with respect to m and tend to small values for large m. Apparently one must be content with the fact that the given sets of weights at discrete times $\Delta\tau$ have Fourier transforms which model the admittance curves with fair approximation, and in that sense are equivalent to the smooth response functions $R(\tau)$ which must exist physically. The residual variances due to regressions of type (7·1) are larger than those in table 10, which were obtained from the individual scattered values.

TABLE 11. WEATHER RESPONSE WEIGHTS FOR ABERDEEN

(The units involved are centimetres of sea level, millibars of air pressure, and 10° units of distance)

function ...	p_{00}	p_{10}	p_{01}	p_{20}	p_{11}	p_{02}
time lag (h)	multipliers $P_m^{(k)}$ to give sea level					
0	1·83	0·64	−0·08	0·13	−0·12	0·16
3	−2·93	−0·90	0·53	−0·21	0·07	0·04
6	1·77	−0·02	−0·49	0·29	−0·30	−0·16
9	−0·94	−0·09	0·07	−0·11	0·27	−0·12
12	−1·31	−0·09	−0·66	0·01	−0·02	−0·28
15	−0·49	0·66	−0·19	−0·15	0·22	−0·13
18	−0·33	−0·45	0·04	−0·08	0·17	0·09
21	3·45	0·50	0·40	0·06	−0·31	0·32
24	−1·56	−0·10	−0·20	−0·09	0·17	−0·16

(*b*) *External surges*

Workers who have concentrated on the generation of surges mainly within the North Sea itself (see, for example, Corkan 1948; Rossiter 1959), have usually had to allow for surges entering the sea as free waves, having been generated elsewhere on the shelf. Such surges have been termed *external surges*. The term is a loose one, because it depends on how wide a sea area the response to one's weather stresses is effective. I have used it in the sense of any

variation of sea level not predicted in terms of the six-component weather function discussed in (*a*). This would include free waves generated west of Ireland or northern Norway, and also anomalies due to errors in the prediction formulae.

The usual way to deal with external surges is to include in one's prediction formulae the observed sea level at a port external to the main sea area. Malin, Stornoway and Lerwick were in fact included in the present analysis mainly for this purpose. Ideally, one can envisage a scheme whereby these three ports form a sort of directionally sensitive array of detectors, such as those used in analysing seismic or short sea waves, to monitor the heights and directions of external waves approaching the north of Scotland. The external surge at Aberdeen would thereby be expressed in terms of a set of response functions including sea levels at perhaps all three stations. However, one has to be careful to distinguish between genuine free waves, and surges which appear at Aberdeen a few hours after Stornoway (say) simply because the weather systems tend to travel eastwards. One way to do this would be to subtract the local weather predictor from each sea level series, and correlate the residuals. In the present case, since the same weather function serves for all stations, it is more convenient to perform a joint correlation analysis between all sea levels involved and the six components of weather. That is, in analysing sea level at Aberdeen, we add cross-spectra involving sea levels at Malin, Stornoway and Lerwick into the formalism (2·11).

The results for residual variance are given in the lowest three rows of table 10, where it is seen that addition of Stornoway and Lerwick do reduce the residual by appreciable amounts, even though the final addition of Malin Head is ineffective. By adding the differences between the fourth and the last rows, the total contribution of the 'external surge' to the variance of sea level at Aberdeen is found to be about 30 cm^2, or 14 % of the total nontidal variance. The irrelevance of Malin Head was confirmed by including it without the other two places, when it gave trivial prediction variances and small and confused admittances. Presumably, Malin Head is too remote to be effectively correlated with Aberdeen when the external surge is truly separated from spurious correlations due to the weather.

The first two panels of figure 10 show the admittances to external surges at Lerwick and Stornoway. The figure is extended to higher frequencies than figure 9 because trends between 1 and 2 c/d are better defined. A clear relationship with both places is evident. However, if the response formula is to be used as a *predictor* in real time, we cannot include any term $\zeta(t)$ without a time lag. This means that the in-phase and out-of-phase admittances X_r and Y_r must be fitted by a formula of type

$$\left.\begin{aligned} X_r &= P_1 \cos\theta_r + P_2 \cos 2\theta_r + \dots \\ Y_r &= -P_1 \sin\theta_r - P_2 \sin 2\theta_r - \dots \end{aligned}\right\} \quad (\theta_r = 2\pi f \Delta\tau). \tag{7·3}$$

Inspection shows that the X, Y values for Lerwick cannot be fitted at low frequencies by such a formula without the constant P_0, corresponding to the unlagged term, added to X_r. This means that an important part of the external surge at Lerwick is simultaneous with sea level at Aberdeen. The result is understandable when one considers a surge progressing from the southwest (figure 1) and taking about the same time to travel from the northern tip of Scotland to Lerwick as the diffracted part to travel down the coast to Aberdeen. An external surge from the north would probably arrive at Lerwick first, but such events are evidently

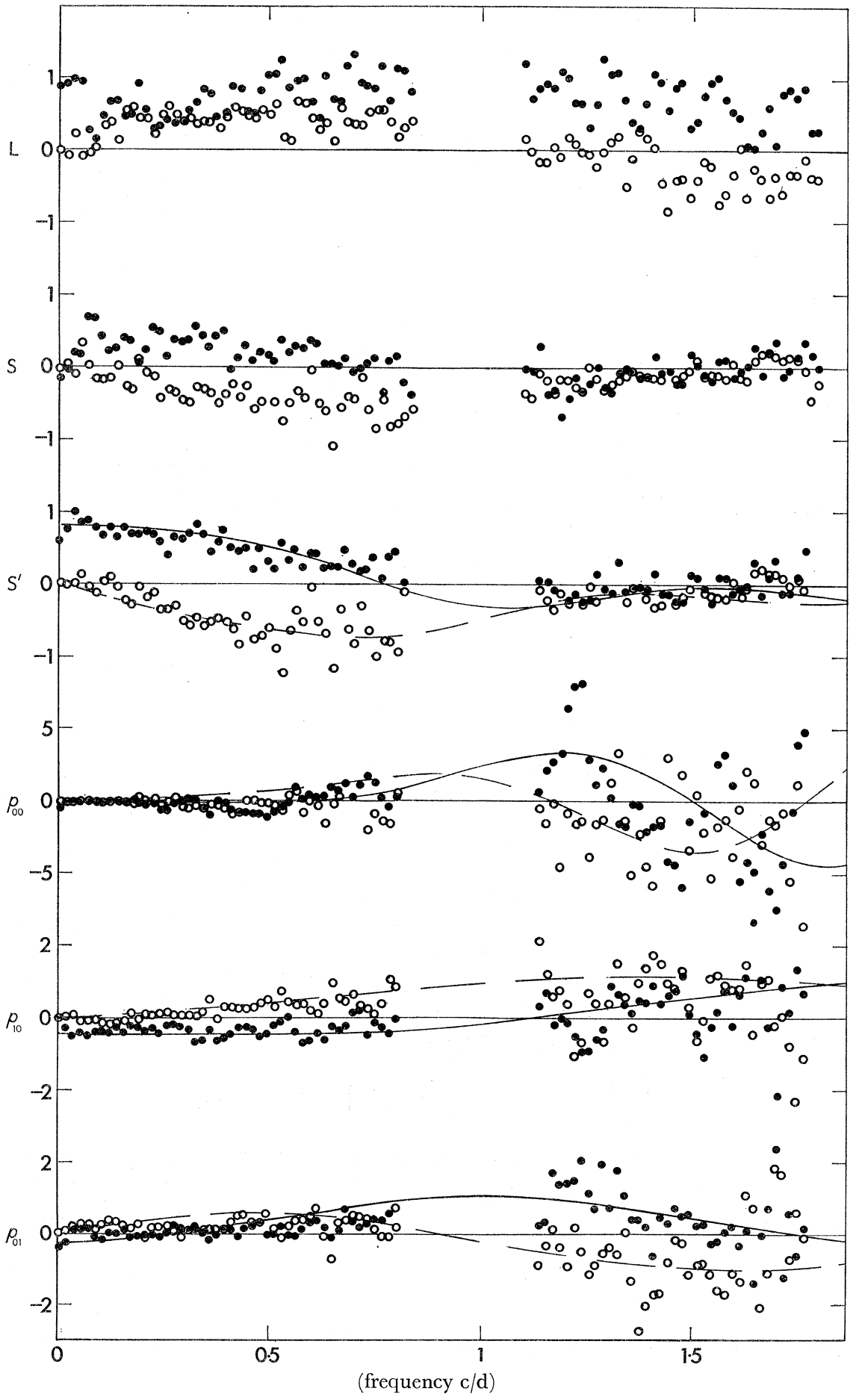

FIGURE 10. Partial admittances of Aberdeen sea level to sea levels at Lerwick and Stornoway (L and S). S' represents Stornoway in the absence of Lerwick. The lowest three panels are the admittances of Aberdeen sea level to pressure coefficients when S' is included. They include in a sense the admittance of Stornoway sea level to weather. Units are as in figure 9.

PHILOSOPHICAL TRANSACTIONS OF THE ROYAL SOCIETY A MATHEMATICAL, PHYSICAL & ENGINEERING SCIENCES

rare, perhaps on account of the dynamical property of Kelvin waves, keeping a coastline to the right (in north latitudes).

Stornoway does not suffer from the defect of Lerwick, since its admittance values in figure 10 can evidently be fitted by positive values of P_r in (7·3). It is therefore the only member of the proposed 'array' to prove useful in the present context. The third panel in figure 10 applies when Stornoway is included on its own, ignoring Lerwick and Malin altogether.

Only the results from the first three pressure coefficients are shown in figure 10. By comparing with figure 9 we see that they are markedly affected by the inclusion of Stornoway sea level. The reason is that the weather here enters as the *difference* between its effects on Aberdeen and Stornoway, which at low frequencies is very small. Therefore all admittances to weather below about 0·5 c/d are of small amplitude in this application. On the other hand, above 1 c/d the effect of Stornoway sea level becomes small, and the weather effects predominate.

External surges predictors were similarly derived for Immingham in terms of Aberdeen sea level, and for Southend in terms of Immingham. The results were similar to the case discussed above.

8. Self prediction

In the preceding sections, the observed sea level has been expressed in an optimum way in terms of tide-generating potentials, the time and space variations of atmospheric pressure and wind (as determined by pressure gradients), and external surges. These, with the effects of tide-surge interaction in shallow water, exhaust our supply of readily predictable processes. The residual variances, of order 100 cm^2, are due to over-simplified formulation, and to neglected physical processes. However, on a basis of short-term prediction, one may reduce the residual variance still further by using immediate past values of the error itself. Self-prediction of low-frequency sea level was shown in M.C. to be more effective and much simpler than a prediction in terms of gravitational and radiational tide potentials, at time lags less than about 5 days (or longer times at Honolulu). Even allowing for 1 or 2 days' observations absorbed in a low-pass filter, the present residuals should be similarly or better suited to the treatment. The spectra at medium-low frequencies (above 1 c/m) have been reduced by the weather predictor, while the very low-frequency (including seasonal) changes in mean sea level, which are largely due to other causes, remain.

As well as low frequency residuals, one may also self-predict the tidal residuals, since these, being also confined to narrow frequency bands, have low frequency *envelopes*. In fact, the near-tidal and seasonal modulations considered in § 6, and high quarter-diurnal noise level at Southend (§ 4 (*b*)) are well suited to self-prediction.

The formal procedure was as follows. I first derived the series of residual sea levels, $\zeta_{\text{res.}}(t)$ say, by subtracting all known prediction forms from $\zeta(t)$. $\zeta_{\text{res.}}$ was then filtered into frequency bands centred on zero and on the tidal species. For simplicity, I used the filters

$$\left.\begin{aligned} \xi_0(t) &= \frac{1}{2N}\sum_{s=-N+1}^{N-1}(1+\cos s\pi/N)\,\zeta_{\text{res.}}(t+s\Delta\tau), \\ \xi_m(t)+\mathrm{i}\eta_m(t) &= \frac{1}{N}\sum_{s=-N+1}^{N-1}(1+\cos s\pi/N)\,\zeta_{\text{res.}}(t+s\Delta\tau)\,\mathrm{e}^{2\pi\mathrm{i}ms\Delta\tau/T} \quad (m\geqslant 1) \end{aligned}\right\} \tag{8·1}$$

with $\Delta\tau = 3$ h, and $T = 1$ lunar day. Only ξ_0 and the semi-diurnal filter $m = 2$ were investigated, with $N = 8$, 16 and 24. The 'real envelope', referred to a future time $(t+t')$,

$$\xi'_m(t,t') = \mathscr{R}[\{\xi_m(t) + i\eta_m(t)\}\, e^{-2\pi i m t'/T}] \quad (t' \geqslant N\Delta\tau) \tag{8·2}$$

is a low frequency variable in t. I therefore tried the autoregressions

$$\tilde{\xi}'_m(t) = \sum_{k=1}^{K} P_{mk}\, \xi'_m(t - kN\Delta\tau, kN\Delta\tau) \tag{8·3}$$

for $m = 0$ and 2, and various numbers of lags, K.

Choise of N is not obvious *a priori*. The filter characteristic of (1) reaches zero at approximately

$$f = \frac{m}{T} \pm \frac{1}{N\Delta\tau},$$

so with $\Delta\tau = 3h$ we must have $N \geqslant 8$ in order to separate the tidal species effectively. If N is large, the envelope (8·2) varies slowly with frequencies of order $(2N\Delta\tau)^{-1}$, but one has a large minimum prediction lag, $N\Delta\tau$. The optimum value depends on the distribution of spectral energy within the filter band. In fact, the predictable variances derived from the best fitted regression (8·3) to residuals from Immingham, listed in table 12, show that the smallest possible value, $N = 8$, gives the best results. The same was found for all stations, and is consistent with the observed fact that the residual noise is concentrated at very low frequencies and close to the tidal bands.

TABLE 12. SELF-PREDICTION VARIANCES (cm²) FOR IMMINGHAM RESIDUALS

	low frequency ($m = 0$)				semi-diurnal ($m = 2$)		
N	K... 1	4	8	N	K... 1	4	8
8	42·1	43·6	44·2	8	29·9	30·0	30·4
16	34·0	35·2	36·5	16	21·6	23·0	23·6
24	28·6	31·4	31·9	24	16·0	16·4	17·3

Table 12 shows another typical result, that the predictable variances increase only very slowly as the number of terms K is increased above 1. For the low frequency case, this was also observed in M.C., where it was suggested that mean sea level behaves statistically like a Markov process. Evidently, the same is true of the 'cusp region' near the semi-diurnal tide.

In actual use, having evaluated the coefficients in (8·3), the regressions $\tilde{\xi}'_m(t)$ are added to the predicted sea levels as an improvement. I used five lags, for arbitrary reasons. The coefficient for $k = 1$ was always much larger than the rest, and a little less than 1. With $K = 5$, $N = 8$, table 13 lists in its first two columns the self-predictable variances for $m = 0$ and 2 at all stations. External surge variables were not used in this calculation. The p.v. for $m = 0$ are similar, as one might expect, while for $m = 2$ they vary greatly, according to the tidal noise level (compare figure 7). The tidal p.v. at Lerwick is almost negligible, because the tidal residual is itself only about 2 cm² (table 5). Roughly speaking the self predictions halve the residual variance in their respective frequency bands.

The third column of table 13 shows the residual variances of the sea level series with only the tide prediction subtracted, while the fourth shows the final residual variances when all, including self and external surge predictors (where appropriate) have been subtracted from

them. The figure of 77 cm^2 for Aberdeen is higher than the sum of the 5th row of table 10, partly because the actual regressions (7·1) for weather give smaller p.v. than the individual admittances at all frequencies on which table 10 is based, and because the self-prediction has its role already partly filled when an external surge sea level is included. As in all analyses, residuals are highest for the shallow water ports, particularly Southend.

TABLE 13. SELF-PREDICTABLE AND RESIDUAL VARIANCES

	self predictions		residuals	
station	$m = 0$	$m = 2$	tide only	total
Malin	87	15	302	79
Stornoway	84	4	311	38
Lerwick	54	1	187	25
Aberdeen	54	11	259	77
Immingham	44	30	361	100
Southend	74	27	510	189

The distribution of residuals for the three North Sea ports is shown in more detail in table 14. The numbers in the second of each pair of columns are those appropriate to a gaussian distribution with the same variance. The observed distributions are fairly symmetrical about the origin, but both large and small errors occur significantly more often than in the normal case. This is probably due to the seasonal variation of intensity of surges. The largest errors were −131 cm at Immingham, and +119 cm at Southend.

TABLE 14. DISTRIBUTION OF ERRORS

	Aberdeen		Immingham		Southend	
range (cm)	observed	normal	observed	normal	observed	normal
< -100	0	0	2	0	0	0
−100 to −80	0	0	2	0	0	0
−80 −60	0	0	5	0	8	0
−60 −40	7	0	14	0	56	16
−40 −20	131	97	180	197	560	617
−20 −10	658	1007	783	1179	1249	1395
−10 0	3424	3240	3272	2968	2481	2316
0 10	3527	3240	3417	2968	2617	2316
10 20	789	1007	834	1179	1289	1395
20 40	137	97	158	197	392	617
40 60	14	0	18	0	27	16
60 80	1	0	2	0	4	0
80 100	0	0	1	0	1	0
> 100	0	0	0	0	4	0
totals	8688	8688	8688	8688	8688	8688

Figures 11·1 and 11·2 compare some 5-day samples of observed and predicted 'tide residuals', that is sea levels from which the pure tide prediction has been subtracted, as presented in most papers about surges. The top two samples of figure 11·1 were selected to show the benefit of self-prediction. In the first, the prediction without self correction is consistently 1 or 2 ft. too high, but the addition of $\tilde{\zeta}'_0(t)$ (possibly with some help from $\tilde{\zeta}'_2(t)$), brings the curves much closer together.

The second panel of 11·1 is a good example of the result of a random tide modulation, such as are responsible for the tidal noise discussed in § 6. Records supplied by the 'Storm

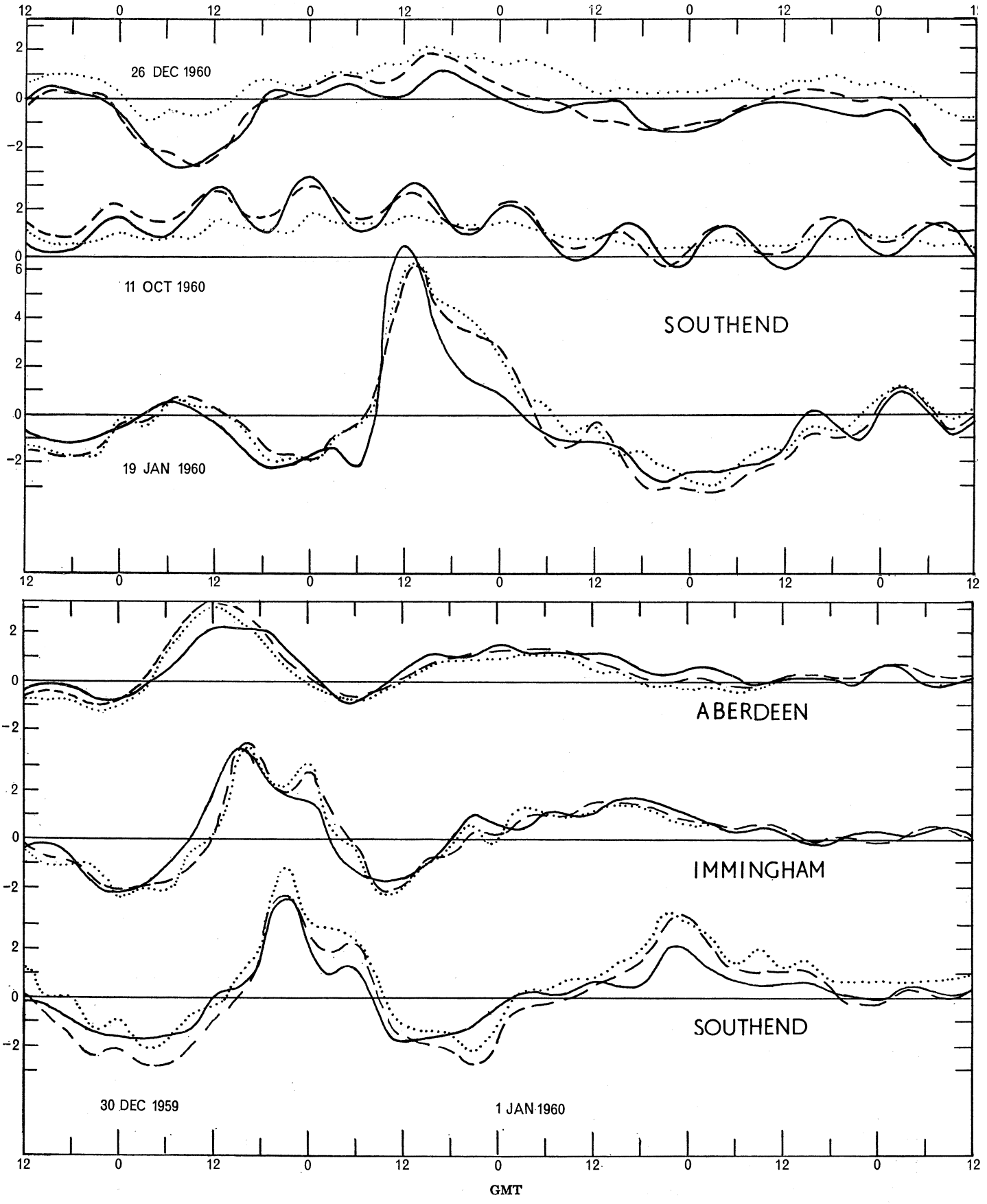

FIGURE 11·1. —, Observed sea levels less (response) tidal predictions for three 5-day periods at Southend. . . ., Sea levels predicted in terms of weather, external surge, and surge-tide interaction only. – – –, The same, with low frequency and tidal self-predictors added. Only the date of the first complete day of each period is given.

FIGURE 11·2. As 11·1, for the same period at three ports.

PHILOSOPHICAL TRANSACTIONS OF THE ROYAL SOCIETY A MATHEMATICAL, PHYSICAL & ENGINEERING SCIENCES

Tide Warning Service' show that the large residual oscillation was widespread in the neighbourhood of the Thames Estuary at the time, and therefore was not the result of a temporary defect in the tide gauge at Southend. Without self prediction, only a small tidal oscillation is predicted. This is due to the surge-tide interaction formula, which evidently accounts correctly for a small part of the modulation, but other physical interactions must also be present, as previously suggested. Since the full modulation changes slowly, the prediction is greatly improved by the inclusion of $\tilde{\zeta}_2'(t)$.

The bottom panel of 11·1 includes the largest surge at Southend during the 3 y period under analysis. Here, the self-prediction has little effect. It sometimes improves and sometimes worsens the comparison, but both predictions are reasonably good. Much the same holds in figure 11·2, where a pair of surges is shown arriving in quick succession at the three North Sea ports. This figure gives a typical impression of the quality of surge predictions by the methods of this paper, without selecting a particularly favourable example. To my knowledge, it compares favourably with, but is not markedly better than the typical product of other methods of surge forecasting in current use.

9. Monthly and fortnightly tides

The analysis of tide gauge records presented in this paper began by identifying the principal tidal motions. To end, I extract some results of unprecedented accuracy for some hitherto neglected tidal motions, by using the weather response functions derived in § 7 (*a*) to reduce the noise level at low frequencies.

The low frequency tides are notoriously difficult to estimate reliably, because they are small and occur in a part of the spectrum where the noise level is high. The harmonic constituents which have received most attention are the elusive Nodal Tide (18·6 years) and the Annual Tide, *Sa*, because they can in principle be extracted from monthly mean sea levels, of which many tens of years' records are available (*Ass. Int. Oceanogr. Phys.* (*U.G.G.I.*) *Pub. Sci.* nos. 5, 10, 12, 19, 20, 21). Monthly means were also used for Haubrich & Munk's (1959) analysis of the stochastic 'Pole Tide' with mean period about 1·2 y. In normal circumstances, the monthly and fortnightly constituents also require some decades of data to extract them from the background noise, but the monthly means are of course useless for such a task. Recently, Wunsch (1966) has made an intensive study of monthly and bimonthly constituents in the Pacific Ocean, extracted from the many years of hourly sea levels stored on magnetic tape at the University of California at La Jolla. He has found that estimates even from 5 or 10 years' data from regions with quiet weather conditions have wide confidence limits in amplitude and phase.

The top part of figure 12 shows the low frequency spectrum of sea level at Lerwick, which has the quietest record of the present data. Even at $\frac{1}{3}$ c/y resolution, the monthly and bimonthly constituents are completely lost in the noise. Only the seasonal component stands out well, but this could be better estimated from the more extensive records of monthly means referred to above. The energy density in the region of 1 c/m is about 5 $\mathrm{cm}^2/(\mathrm{c/y})$. If *Mm* has an amplitude of 1·1 cm, its variance is 0·6 cm^2. So to obtain a filter at 1 c/m with noise energy content one-third that of the tidal signal we should require $5 \times 3/0{\cdot}6 = 25$ y of raw sea level data. *Mf* would require considerably less time for the same ratio, and it should

be remarked that the period 1959–61 is particularly unfavourable to the determination of the fortnightly tide, because the range of lunar declination is at its least, the Moon's Ascending Node being near the Autumnal Equinox. Around 1951 or 1969 the fortnightly tidal energy would be more than four times as great.

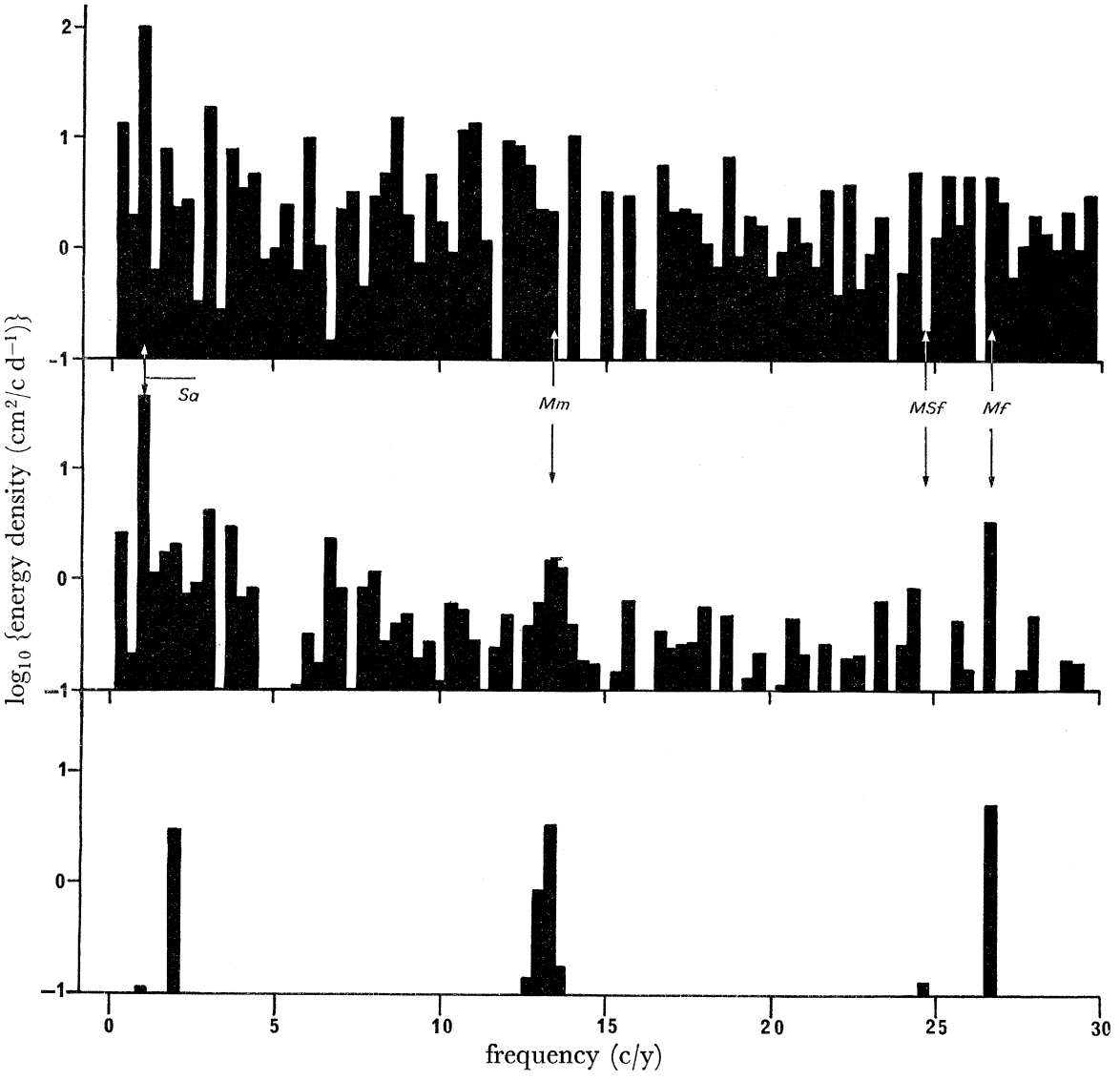

FIGURE 12. Top diagram: Low frequency spectrum of Lerwick sea level. Middle diagram: The same, when response to weather is subtracted. Bottom diagram: Spectrum of zonal gravitational potential a_2^0. Resolution in all diagrams is 1 cycle per 1093 days.

The middle panel of figure 11 shows the spectrum of the same record after subtraction of the noise coherent with the six-component weather series described in § 7 (*a*). No other sea level record was included to allow for 'external surge' (§ 7 (*b*)), as this would have distorted, if not removed the tidal effects sought, whereas a monthly periodicity in the weather is practically nonexistent. We see that the noise level is drastically reduced, and the monthly and bi-monthly tides now stand clear. The same sort of results obtained for Malin, Stornoway and Aberdeen, but at Immingham and Southend the residual noise level was still too

high for the tides to stand out, even though their predictable variances due to weather were equally or even more effective (see table 13).

The lowest panel shows the spectrum of the simultaneous zonal gravity potential a_2^0, which is the principal driving agent for these tides. As in the spectrum of weather-free sea level, the component at 2 c/m is well resolved at the 80th harmonic of 1093 days, but the monthly component is spread over a group around the 40th harmonic, since it varies with the period of perigee, an anomalistic month. The other strong component of a_2^0 is at 2 c/y, but its counterpart in the sea level spectrum is confused with radiational effects, and noise which is not removed with the atmospheric pressure. At Malin, a nonlinear effect was observed in the constituent known as *MSf*, manifestly absent from the Lerwick spectrum and also from Aberdeen and Stornoway. *MSf* is chiefly due to an interaction between M_2 and S_2, which therefore distorts *Mm* through M_2 and N_2, and *Mf* through M_2 and K_2. These distortions were corrected accordingly. The interaction coefficient is†

$$Z(2, -2) = (-4{\cdot}5 + 0{\cdot}6\mathrm{i}) \times 10^{-4}\,\mathrm{cm}^{-1},$$

so its general effect is to depress sea level at spring tides. This may well be due to the centrifugal effect of tidal currents round Malin Head itself. It must also depress overall mean sea level by a few centimetres.

By correlating the residual spectra with the spectrum of a_2^0, using ensemble averages over the groups of harmonics 38 to 42 and 78 to 82, I obtained linear relationships with the zonal equilibrium tide (at 58° N), together with estimates of coherence, from which standard deviations were derived. All relevant results are listed in table 15, where the group numbers (0, *N*) refer to *N* c/m, and the amplitude ratio and phase lags refer to the equilibrium tide. *H* is the 'constituent amplitude' in the notation of harmonic tidal analysis.

TABLE 15. RESULTS OF MONTHLY AND FORTNIGHTLY ANALYSES

	Lerwick		Stornoway		Aberdeen		Malin	
tidal group	0 1	0 2	0 1	0 2	0 1	0 2	0 1	0 2
ampl. ratio	0·86	1·00	1·03	0·93	0·94	0·92	0·89	1·18
phase lag	1°	6°	−2°	22°	18°	29°	−13°	52°
coherence	0·52	0·92	0·67	0·80	0·42	0·88	0·40	0·60
s.d. (ampl.)	0·26	0·09	0·23	0·15	0·35	0·11	0·39	0·26
s.d. phase	15°	5°	13°	9°	20°	6°	22°	16°
H (cm)	1·1	2·4	1·3	2·3	1·2	2·2	1·1	2·9

The results are all consistent with an amplitude ratio of about 1 with a few degrees phase lag. This ratio is high, since elastic yielding of the Earth's crust should reduce the effective tide by about 30 %. Proudman (1960), in an argument based on frictional dissipation, considered that a month or fortnight was too short for static response. Wunsch (1966) has re-examined low frequency solutions of Laplace's equations in a rectangular inviscid β-plane ocean, and finds them to contain hitherto unsuspected variations in longitude and latitude with scales of order 1000 miles. The variations were comparable with the variations in his measurements at Pacific Islands, though his model was too idealized for exact comparison. Some of Wunsch's measured amplitude ratios were in fact near 1, but his theoretical model allowed such values only to the west of centre of the basin; towards the east, amplitudes were

† In view of the bad behaviour of the gauge at Malin in 1959–60, (§ 6), this coefficient was confirmed by analysing the record during 1961 only.

theoretically small. However, at San Francisco on the east side of the Pacific, both monthly and fortnightly tides had amplitude ratios greater than 1. The present results confirm that a realistic theory of the lower frequency tides must allow large amplitudes at the eastern boundaries.

10. Concluding remarks

In this paper, a good deal of information has been extracted from relatively short records of sea level. The information can be divided into three categories:

(i) Factual information about the physical nature of tides and surges, their admittances to exciting forces, their modulations, and interactions.

(ii) Applicability of techniques of analysis, such as those involving the bispectrum, multiple correlation with weather variables, and self-prediction, most of which have apparently not been tried before with sea levels.

(iii) Results of potentially practical use in forecasting.

Much of the factual material is offered without much attempt at theoretical explanation. This is partly on account of the diversity of the ground covered, and partly because the observed features evidently depend upon details of coastal and bottom topography, possibly over a wide area. The major features of tides and surges in the North Sea have been known for many years, and can be reproduced roughly by simplified analytical models. One could only hope to reproduce some of the finer details, such as the surge-tide interactions, by laborious numerical solution of the nonlinear wave equations with realistic boundaries. (Some such efforts, by the University of Liverpool Tidal Institute, have already been referred to.) Some features, in fact suggest special subjects of research. Is the similarity of interaction at Immingham and Southend, for example, due to both ports being in estuaries, or are they part of a coherent pattern in the whole of the southern North Sea? Is the low frequency tidal modulation due to oceanic, local, or instrumental peculiarities?

The techniques have proved successful on the whole, but the scatter in such figures as 5 and 9 show that a good deal more than three years' data is necessary to achieve definitive results. At the same time, some scatter may be due to imprecise physical assumptions such as the implied linearization of wind stress. A crucial test would be to ascertain whether the amplitude of the scatter is halved if estimated from 12 years' data. Any measure which led to smoother sequences of response weights would also mark an improvement.

The practical possibilities of the response formulae for forecasting sea levels a few hours ahead are obvious, but they have not been the principal objective of this work. The authorities concerned with tide and surge predictions in various countries have their own methods and formulae which serve their purpose well. The methods could hardly be applied to surge prediction in real time without the use of an automatic computer 'on-line', and this may have practical disadvantages. For this reason, and for others stated above, I have not taken the considerable space necessary to list all the response weights for various combinations of weather and external surge variables. However, I will gladly supply any set of numbers on personal request.

Some difficulty might be experienced in applying the surge-tide interaction formula (5·1). It was evaluated in terms of nontidal sea level at the port itself, but since it involves a value

of $\zeta(t)$ at the time of prediction $t = 0$, at least this value would have to be supplied in practice from an independent surge formula. How far errors in the surge prediction affect the accuracy of the interaction formula is a matter for special research.

I should like to acknowledge valuable discussions on different parts of this work with Walter H. Munk, J. R. Rossiter, and various members of the British Advisory Committee on Oceanographic and Meteorological Research. I am also grateful to the British and Irish Ordnance Surveys, the Hydrographic Department of the Ministry of Defence, the British Transport Docks Board (Grimsby), and the Port of London Authority, for the supply of tide gauge charts. Most of the purely tidal computations were done by the C.D.C. 3600 computer of the University of California at La Jolla. The rest of the work used the I.B.M. 7094 at the 'I.B.M. Data Centre', London.

References

Bowden, K. F. 1956 The flow of water through the Straits of Dover. *Phil. Trans.* A **248**, 517–551.

Bullard, E. C., Oglebay, F. E., Munk, W. H. & Miller, G. R. 1966 *A user's guide to BOMM.* (2nd. ed.) University of California, La Jolla.

Charnock, H. & Crease, J. 1957 Physical oceanography—North Sea surges. *Sci. Prog.* **45**, 494–511.

Corkan, R. H. 1934 An annual perturbation in the range of tide. *Proc. Roy. Soc.* A **144**, 537–559.

Corkan, R. H. 1948 Storm surges in the North Sea. *H.O. Misc.*, no. 15072, *Washington, D.C.* **1**, 1–170; **2**, 171–336.

Darbyshire, J. & Darbyshire, M. 1956 Storm surges in the North Sea during the winter 1953–4. *Proc. Roy. Soc.* A **235**, 260–274.

Dietrich, G., Wyrtki, K., Carruthers, J. N., Lawford, A. L. & Parmenter, H. C. 1952 *Wind conditions over the seas around Britain 1900–1949*, 38 pp. D. H. I., Hamburg.

Doodson, A. T. 1924 Meteorological perturbations of sea level and tides. *Mon. Not. R. Astr. Soc. Geophys. Suppl.* **1** (4), 124–147.

Hamon, B. V. 1966 Continental shelf waves and the effects of atmospheric pressure and wind stress on sea level. *J. Geophys Res.* **71** (12), 2883–2893.

Hansen, W. 1956 Theorie zur Errechnung des Wasserstandes und der Strömungen in Randmeeren nebst Anwendungen. *Tellus* **8** (3), 287–300.

Hasselmann, K., Munk, W. & Macdonald, G. 1963 Bispectra of ocean waves. Ch. 8 of *Time series analysis* (Ed. Rosenblatt, M.). London: J. Wiley and Sons.

Haubrich, R. & Munk, W. 1959 The pole tide. *J. Geophys. Res.* **64** (12), 2373–2388.

Ishiguro, S. 1966 Storm surges in the North Sea—an electronic model approach. *Report 4. National Institute of Oceanography.*

Ishiguro, S. 1962 An electronic analogue method for tides and storm surges. Pp. 265–269 of *Proc. Symp. math.-hydro. methods of phys. oceanography.* (Ed. Hansen, W.). Univ. Hamburg.

Lamb, H. 1932 *Hydrodynamics* (6th ed.). Cambridge University Press.

Lennon, G. W. & Rossiter, J. R. 1967. An intensive study of tidal data in the Thames Estuary. *Symposium on Tides, Monaco*, April 1967.

Munk, W. H. & Bullard, E. C. 1963 Patching the long-wave spectrum across the tides. *J. Geophys. Res.* **68** (12), 3627–3634.

Munk, W. H. & Cartwright, D. E. 1966 Tidal spectroscopy and prediction. *Phil. Trans.* A **259**, 533–581.

Munk, W. H., Zetler, B. & Groves, G. W. 1965 Tidal cusps. *Geophys J., R. Astr. Soc.* **10** (2), 211–219.

Proudman, J. 1957 Oscillations of tide and surge in an estuary of finite length. *J. Fluid Mech.* **2** (4), 371–382.

PHILOSOPHICAL TRANSACTIONS OF THE ROYAL SOCIETY A MATHEMATICAL, PHYSICAL & ENGINEERING SCIENCES

Proudman, J. 1960 The condition that a long-period tide shall follow the equilibrium law. *Geophys J., R. Astr. S.* **3** (2), 244–249.

Robinson, A. R. 1964 Continental shelf waves and the response of sea level to weather systems. *J. Geophys. Res.* **69** (2), 367–368.

Rossiter, J. R. 1959 Research on methods of forecasting storm surges on the east and south coasts of Great Britain. *Quart. J. R. Met. Soc.* **85**, 262–277.

Rossiter, J. R. 1961 Interaction between tide and surge in the Thames. *Geophys J., R. Astr. Soc.* **6** (1), 29–53.

Sheppard, P. A. 1958 Transfer across the Earth's surface and through the air above. *Quart. J. R. Met. Soc.* **84**, 205–224.

Tucker, M. J. 1963 Physical oceanography—long waves in the sea. *Sci. Prog.* **51**, 413–424.

Welander, P. 1961 Numerical prediction of storm surges. *Adv. Geophys.* **8**, 315–379.

Wunsch, C. I. 1966 On the scale of the long-period tides. Ph.D. Thesis, Massachusetts Inst. Tech. (unpublished).

Zetler, B. D. & Cummings, R. A. 1967 A harmonic method for predicting shallow-water tides. *J. Mar. Res.* **25** (1), 103–114.

Appendix A

Complete list of tidal response weights, as described in text. The symbols on the left represent the appropriate tidal variable with argument $(t-s\Delta\tau)$ with $\Delta\tau = 2$ days. $(\tilde{\zeta}^{\mathrm{I}})^{j\pm k}$ represents the product of two first-order tidal forms of species j and k (conjugate for $-$ sign), as given by the first five rows of weights for each port.

Malin Head

First order weights

variable	s	P	Q	variable	s	P	Q
c_2^1	2	0·6505	0·0230	c_2^2	2	0·1776	0·2727
	1	−0·7675	−0·0296		1	1·1820	1·0657
	0	0·2100	0·3038		0	−2·9284	−3·7831
	−1	0·3415	−0·2352		−1	−0·8321	3·7941
	−2	−0·1909	0·0311		−2	1·1454	−0·6369

Main set

c_2^1	2	0·5614	0·1717	c_2^2	2	1·0538	0·0737
	1	−0·3587	−0·2812		1	−1·6860	−1·4471
	0	−0·2341	0·3535		0	−2·4637	2·5759
	−1	0·4987	−0·1846		−1	2·4290	0·0375
	−2	−0·2204	0·0135		−2	−0·4530	−0·6584
c_3^1	0	1·7554	1·0683	c_3^2	0	1·9254	0·9065
$(\tilde{\zeta}^{\mathrm{I}})^{2-1}$	0	−1·5	$4·9\times10^{-4}$	χ_2^2	0	0·0060	11·1202
$(\tilde{\zeta}^{\mathrm{I}})^{1+2-2}$	0	1·7	$3·6\times10^{-6}$	$(\tilde{\zeta}^{\mathrm{I}})^{2+2-2}$	0	1·9	$3·2\times10^{-6}$
c_3^3	1	2·3510	1·0205	$(\tilde{\zeta}^{\mathrm{I}})^{2+2}$	0, 0	−3·2	$4·0\times10^{-4}$
	0	0·4019	2·2405		0, $\frac{1}{2}$	4·9	−10·7
	−1	0·5521	0·6281		$\frac{1}{2}$, $\frac{1}{2}$	−0·9	8·2
$(\tilde{\zeta}^{\mathrm{I}})^{2+1}$	0	−8·1	$2·7\times10^{-4}$	$(\tilde{\zeta}^{\mathrm{I}})^{2+2+1}$	0	1·5	$1·2\times10^{-6}$
$(\tilde{\zeta}^{\mathrm{I}})^{2+2-1}$	0	−2·0	$1·7\times10^{-6}$	$(\tilde{\zeta}^{\mathrm{I}})^{2+2+2}$	0	−0·2	$0·1\times10^{-6}$

Stornoway

First order weights

c_2^1	2	0·5059	0·5153	c_2^2	2	0·4095	0·4480
	1	−0·4023	−0·5644		1	1·1325	−0·0641
	0	−0·0918	0·5202		0	−4·7552	−1·1868
	−1	0·4128	−0·2446		−1	1·5094	3·2997
	−2	−0·1951	0·0486		−2	0·4987	−1·0719

STORNOWAY (*cont.*)

variable	s	P	Q	variable	s	P	Q
			Main set				
c_2^1	2	0·4181	0·6245	c_2^2	2	1·2045	−0·1326
	1	−0·0123	−0·7192		1	−2·4089	−1·4929
	0	−0·4755	0·4491		0	−2·6495	4·4748
	−1	0·4951	−0·1206		−1	3·5355	−0·8802
	−2	−0·1877	0·0178		−2	−0·9788	−0·7121
c_3^1	0	1·6135	1·4365	c_3^2	0	2·0530	0·8998
$(\tilde{\zeta}^{\mathrm{I}})^{2-1}$	0	−3·3	$2{\cdot}1\times10^{-4}$	χ_2^2	0	11·0214	10·1732
$(\tilde{\zeta}^{\mathrm{I}})^{1+2-2}$	0	1·4	$1{\cdot}4\times10^{-6}$	$(\tilde{\zeta}^{\mathrm{I}})^{2+2-2}$	0	0·6	$1{\cdot}1\times10^{-6}$
c_3^3	1	2·8731	−2·9382	$(\tilde{\zeta}^{\mathrm{I}})^{2+2}$	0, 0	−11·6	$3{\cdot}1\times10^{-4}$
	0	−4·0579	3·7461		0, $\frac{1}{2}$	26·9	−13·0
	−1	2·4975	1·2881		$\frac{1}{2}$, $\frac{1}{2}$	−15·2	14·4
$(\tilde{\zeta}^{\mathrm{I}})^{2+1}$	0	−3·1	$4{\cdot}4\times10^{-4}$	$(\tilde{\zeta}^{\mathrm{I}})^{2+2+1}$	0	−0·4	$-0{\cdot}1\times10^{-6}$
$(\tilde{\zeta}^{\mathrm{I}})^{2+2-1}$	0	−0·5	$-0{\cdot}3\times10^{-6}$	$(\tilde{\zeta}^{\mathrm{I}})^{2+2+2}$	0	0·1	$0{\cdot}2\times10^{-6}$

LERWICK

			First order weights				
c_2^1	2	0·4000	−0·1285	c_2^2	2	0·1182	−0·3053
	1	−0·4066	0·4339		1	−0·4116	−0·1368
	0	0·3514	−0·2560		0	0·9794	1·6590
	−1	−0·1521	−0·0826		−1	0·3697	−1·1978
	−2	0·0033	0·1110		−2	−0·3562	0·1403
			Main set				
c_2^1	2	0·2905	−0·0989	c_2^2	2	−0·2603	0·0521
	1	−0·1672	0·4489		1	1·2215	0·2005
	0	0·0238	−0·3683		0	−0·1686	−0·3729
	−1	0·0911	0·1189		−1	−0·2475	0·4044
	−2	−0·0509	−0·0236		−2	0·1812	0·0270
c_3^1	0	1·4524	0·7424	c_3^2	0	−0·4267	−0·6605
$(\tilde{\zeta}^{\mathrm{I}})^{2-1}$	0	1·5	$4{\cdot}2\times10^{-4}$	χ_2^2	0	−2·2672	−7·5911
$(\tilde{\zeta}^{\mathrm{I}})^{1+2-2}$	0	−1·2	$-0{\cdot}6\times10^{-6}$	$(\tilde{\zeta}^{\mathrm{I}})^{2+2-2}$	0	2·2	$-2{\cdot}2\times10^{-6}$
c_3^3	1	−0·5403	−1·2307	$(\tilde{\zeta}^{\mathrm{I}})^{2+2}$	0, 0	2·4	$-11{\cdot}1\times10^{-4}$
	0	−0·1496	0·9944		0, $\frac{1}{2}$	−1·6	25·1
	−1	0·2980	−0·1176		$\frac{1}{2}$, $\frac{1}{2}$	−1·5	−18·2
$(\tilde{\zeta}^{\mathrm{I}})^{2+1}$	0	−6·1	$2{\cdot}3\times10^{-4}$	$(\tilde{\zeta}^{\mathrm{I}})^{2+2+1}$	0	−0·8	$3{\cdot}0\times10^{-6}$
$(\tilde{\zeta}^{\mathrm{I}})^{2+2-1}$	0	−0·7	$3{\cdot}9\times10^{-6}$	$(\tilde{\zeta}^{\mathrm{I}})^{2+2+2}$	0	5·2	$-1{\cdot}0\times10^{-}$

ABERDEEN

			First order weights				
c_2^1	2	0·7131	−0·7144	c_2^2	2	−0·9033	−0·3003
	1	−1·1419	1·2722		1	0·8070	−0·2706
	0	1·3221	−0·8248		0	0·9369	−0·0130
	−1	−0·9032	0·0778		−1	0·4272	−0·7899
	−2	0·3056	0·0939		−2	−0·5107	0·0641
			Main set				
c_2^1	2	0·5564	−0·5251	c_2^2	2	−0·8251	0·2822
	1	−0·7236	1·0479		1	1·6792	−0·6390
	0	0·7502	−0·6277		0	0·9336	−1·3226
	−1	−0·3555	0·0320		−1	−0·9112	−0·0397
	−2	0·0623	−0·0100		−2	0·1255	0·3126
c	0	2·6179	−0·3950	c_3^2	0	−2·0823	−2·6217
$(\tilde{\zeta}^{\mathrm{I}})^{2-1}$	0	3·6	$1{\cdot}4\times10^{-4}$	χ_2^2	0	−9·8486	−2·0288
$(\tilde{\zeta}^{\mathrm{I}})^{1+2-2}$	0	0·1	$0{\cdot}3\times10^{-6}$	$(\tilde{\zeta}^{\mathrm{I}})^{2+2-2}$	0	−2·5	$0{\cdot}2\times10^{-6}$
c_3^3	1	−2·0344	2·3409	$(\tilde{\zeta}^{\mathrm{I}})^{2+2}$	0, 0	−4·1	$2{\cdot}0\times10^{-4}$
	0	3·2867	−1·3996		0, $\frac{1}{2}$	7·8	−4·7
	−1	−2·0416	−1·0193		$\frac{1}{2}$, $\frac{1}{2}$	−5·4	3·3
$(\tilde{\zeta}^{\mathrm{I}})^{2+1}$	0	−1·6	$2{\cdot}9\times10^{-4}$	$(\tilde{\zeta}^{\mathrm{I}})^{2+2+1}$	0	−0·3	$0{\cdot}8\times10^{-6}$
$(\tilde{\zeta}^{\mathrm{I}})^{2+2-1}$	0	−1·4	$0{\cdot}1\times10^{-6}$	$(\tilde{\zeta}^{\mathrm{I}})^{2+2+2}$	0	0·2	$-0{\cdot}2\times10^{-6}$

PHILOSOPHICAL TRANSACTIONS OF THE ROYAL SOCIETY A MATHEMATICAL, PHYSICAL & ENGINEERING SCIENCES

IMMINGHAM

variable	s	P	Q	variable	s	P	Q
			First order weights				
c_2^1	2	−0·1666	−1·6140	c_2^2	2	0·3551	2·5628
	1	−0·2311	2·3408		1	−0·9035	−4·8800
	0	0·9004	−1·7221		0	−4·9451	7·5732
	−1	−0·9792	0·7782		−1	5·5644	−4·2121
	−2	0·4498	−0·2077		−2	−2·2099	0·2734
			Main set				
c_2^1	2	−0·1144	−1·3774	c_2^2	2	−1·0797	1·0690
	1	0·1998	1·9513		1	0·8327	2·1691
	0	0·3254	−1·2494		0	−3·0933	−3·8364
	−1	−0·5185	0·1919		−1	−0·3131	1·9782
	−2	0·1398	0·0523		−2	0·2023	0·0448
c_3^1	0	0·5830	−3·2526	c_3^2	0	1·9887	0·9333
$(\tilde{\zeta}^{\mathrm{I}})^{2-1}$	0	−1·2	$1·9\times10^{-4}$	χ_2^2	0	27·2446	−9·8910
$(\tilde{\zeta}^{\mathrm{I}})^{1+2-2}$	0	−1·6	$-2·6\times10^{-6}$	$(\tilde{\zeta}^{\mathrm{I}})^{2+2-2}$	0	−2·2	$-1·6\times10^{-6}$
c_3^3	1	−0·9155	−2·1352	$(\tilde{\zeta}^{\mathrm{I}})^{2+2}$	0, 0	1·3	$1·9\times10^{-4}$
	0	3·7640	2·0611		0, ½	−2·6	−0·0
	−1	0·7214	−3·5438		½, ½	0·1	−0·7
$(\tilde{\zeta}^{\mathrm{I}})^{2+1}$	0	3·0	$4·1\times10^{-4}$	$(\tilde{\zeta}^{\mathrm{I}})^{2+2+1}$	0	0·6	$-0·9\times10^{-6}$
$(\tilde{\zeta}^{\mathrm{I}})^{2+2-1}$	0	−1·4	$-0·2\times10^{-6}$	$(\tilde{\zeta}^{\mathrm{I}})^{2+2+2}$	0	0·2	$-0·0\times10^{-6}$

SOUTHEND

variable	s	P	Q	variable	s	P	Q
			First order weights				
c_2^1	2	−1·8211	−0·2681	c_2^2	2	−0·9445	−2·0676
	1	2·8266	1·4334		1	5·6552	2·6637
	0	−1·9474	−2·2674		0	−6·1282	−10·7322
	−1	0·6724	1·8169		−1	0·1558	12·0851
	−2	−0·0496	−0·7163		−2	2·5690	−3·4642
			Main set				
c_2^1	2	−1·4695	−0·3812	c_2^2	2	0·0049	−2·0725
	1	2·2589	0·9808		1	1·6884	0·3648
	0	−1·4719	−1·6078		0	0·4110	−3·2260
	−1	0·1830	1·3574		−1	−0·3783	3·6950
	−2	0·1615	−0·4161		−2	0·7245	−1·5301
c_3^1	0	−1·9317	−1·7445	c_3^2	0	3·8076	1·0627
$(\tilde{\zeta}^{\mathrm{I}})^{2-1}$	0	1·0	$5·2\times10^{-4}$	χ_2^2	0	−8·9923	32·1374
$(\tilde{\zeta}^{\mathrm{I}})^{1+2-2}$	0	−3·0	$-3·2\times10^{-6}$	$(\tilde{\zeta}^{\mathrm{I}})^{2+2-2}$	0	−6·3	$-1·6\times10^{-6}$
c_3^3	1	5·1101	1·5242	$(\tilde{\zeta}^{\mathrm{I}})^{2+2}$	0, 0	−10·1	$-9·1\times10^{-4}$
	0	−3·2716	0·3758		0, ½	30·2	7·5
	−1	4·3625	2·7893		½, ½	−16·3	2·0
$(\tilde{\zeta}^{\mathrm{I}})^{2+1}$	0	3·8	$10·4\times10^{-4}$	$(\tilde{\zeta}^{\mathrm{I}})^{2+2+1}$	0	−1·4	$-0·0\times10^{-6}$
$(\tilde{\zeta}^{\mathrm{I}})^{2+2-1}$	0	−2·3	$-1·9\times10^{-6}$	$(\tilde{\zeta}^{\mathrm{I}})^{2+2+2}$	0	0·4	$-0·5\times10^{-6}$

APPENDIX B

Surge-tide interaction weights for equation (5·5). s refers to time lags $s\Delta\tau$, where $\Delta\tau = 3$ h. P_2 and Q_2 are in units cm^{-1}, P_3, Q_3 in cm^{-2}.

IMMINGHAM

s	10^4P_2	10^4Q_2	$10^6\times P_3^+$	$10^6Q_3^+$	$10^6P_3^-$
4	0·4506	−2·4321	1·2284	−0·7250	−1·3906
3	−1·7421	3·1889	−1·7519	2·1075	3·7001
2	1·4283	−2·0713	3·1996	−2·4689	−3·7695
1	−1·8045	2·3743	−2·4413	3·3488	5·3693
0	0·7774	1·1322	0·8329	−2·2407	−4·2922

SOUTHEND

s	$10^4 P_2$	$10^4 Q_2$	$10^6 P_3^+$	$10^6 Q_3^+$	$10^6 P_3^-$
4	0·9187	1·6974	3·5552	−0·9777	0·0637
3	−1·3325	−7·9472	−6·3090	1·8347	−0·0964
2	−0·3580	11·2188	8·5800	−4·0329	2·3158
1	−0·7324	−8·4647	−6·7774	5·1937	1·3170
0	0·2542	8·3323	1·6306	−3·8770	−4·1251

APPENDIX C

Polynomial approximation to $x|x|$

Since the function $f(x) = x|x|$ is odd, any polynomial approximation to it must contain odd powers of x only. A perfect equality between $f(x)$ and

$$k_1 x + k_3 x^3 + k_5 x^5 + \ldots$$

is impossible, if only because it is clearly impossible to match the second derivative at $x = 0 \pm \epsilon$. However, using the property that x varies in time such that large positive or negative values are increasingly rare with magnitude, we may approximate on the criterion that the *time-mean squared difference* is minimized. That is, we seek to minimize

$$\int_{-\infty}^{\infty} \left[f(x) - \sum_{n=1}^{2N-1} c_n P_n(x) \right]^2 g(x)\, \mathrm{d}x \qquad (\mathrm{A}\,1)$$

with respect to its coefficients c_n, where $P_n(x)$ is a convenient set of polynomials, and $g(x)$ is the frequency distribution of x in time. The *precise* form of $g(x)$ is unimportant, and it is convenient to assume a Gaussian distribution, $g(x) = (1/\sqrt{\pi}\bar{a})\, \mathrm{e}^{-x^2/\bar{a}^2}$, where $\bar{a}$ is the amplitude of a pure sine wave with the same variance $(\frac{1}{2}\bar{a}^2)$ as x. Then

$$\int_{-\infty}^{\infty} P_m(x) \left[f(x) - \sum_{1}^{2N-1} c_n P_n(x) \right] \mathrm{e}^{-x^2/\bar{a}^2}\, \mathrm{d}x = 0 \quad (m = 1, 3, 5, \ldots, 2N-1).$$

This equation is immediately solved by choosing $P_n(x)$ to be the set of Hermite polynomials $H_n(\xi)$, $\xi = x/\bar{a}$, where

$$H_0(\xi) = 1, \quad H_1(\xi) = 2\xi, \quad H_{n+1} = 2\xi H_n - 2nH_{n-1}.$$

Then

$$\int_{-\infty}^{\infty} P_m(x)\, P_n(x)\, \mathrm{e}^{-x^2/\bar{a}^2}\, \mathrm{d}x = 0 \quad \text{for all} \quad m \neq n,$$

and

$$c_n = \frac{2\bar{a}^2}{2^n n!\sqrt{\pi}} \int_0^{\infty} \xi^2 H_n(\xi)\, \mathrm{e}^{-\xi^2}\, \mathrm{d}\xi \quad (n = 1, 3, 5, \ldots, 2N-1).$$

Finally, one finds

$$f(x) \doteqdot \frac{\bar{a}^2}{\sqrt{\pi}} \Big[2\xi + \tfrac{1}{12}(8\xi^3 - 12\xi) - \tfrac{1}{480}(32\xi^5 - 160\xi^3 + 120\xi) + \ldots - \left(\frac{-1}{2}\right)^{N-1} \left(\frac{1 \cdot 3 \cdot 5 \ldots (2N-5)}{(2N-1)!} \right) H_{2N-1}(\xi) \Big], \qquad (\mathrm{A}\,2)$$

and the mean square difference (A 1) for N terms is

$$D^2 = \bar{a}^4 \left[\frac{3}{4} - \frac{2}{\pi} \left\{ 1 + \tfrac{1}{6} + \tfrac{1}{120} + \ldots + \left(\frac{1^2 \cdot 3^2 \cdot 5^2 \ldots (2N-5)^2}{(2N-1)!} \right) \right\} \right]. \qquad (\mathrm{A}\,3)$$

D^2 tends to zero as N tends to infinity.

Some r.m.s. differences from A 3 are:

N	$D/\bar{a}^2$
1	0·3367
2	0·0853
3	0·0444
4	0·0289

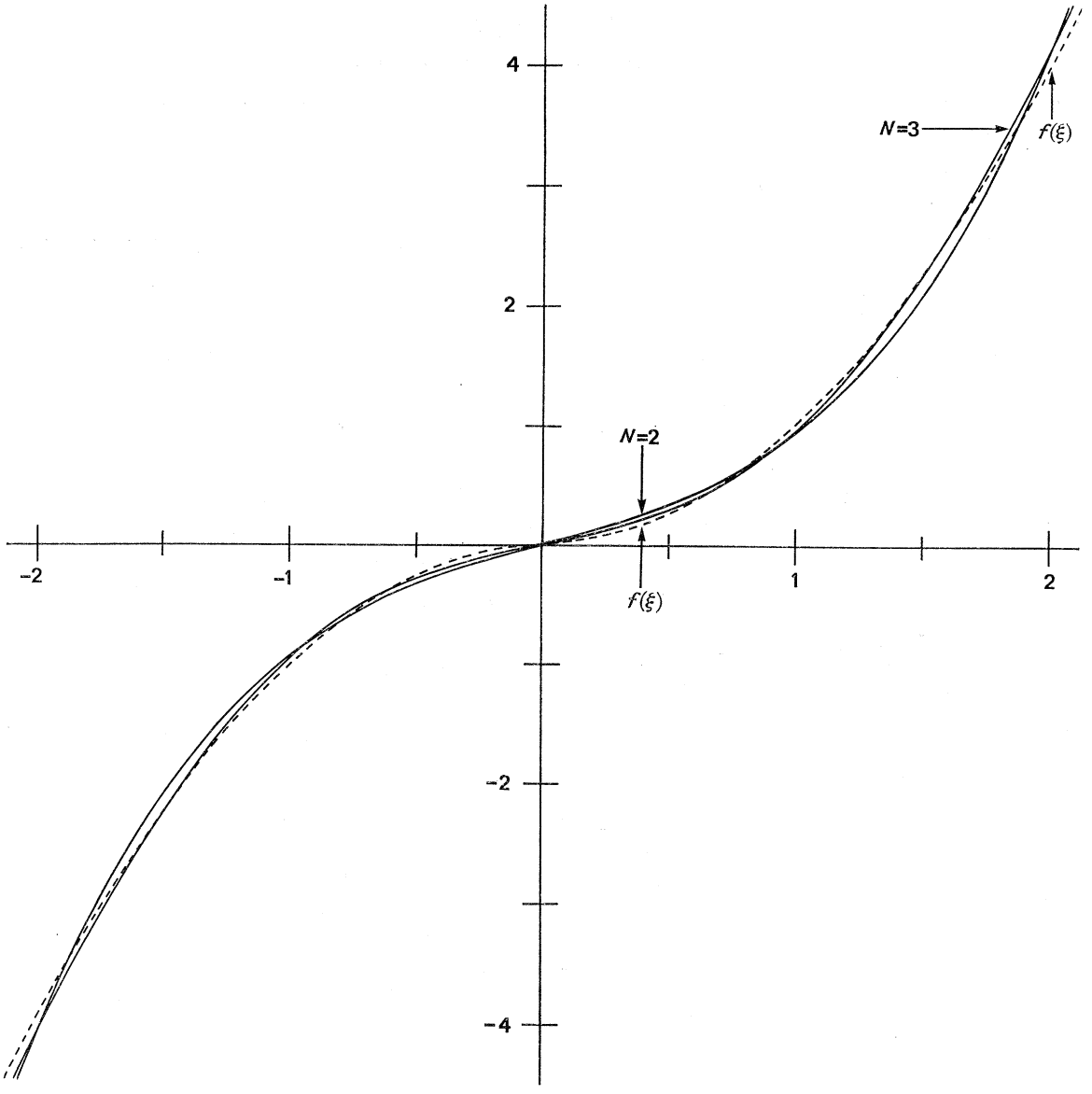

FIGURE 13. Polynomial approximations (A 2) to $\xi|\xi|$ (– – –) with $N = 2$ and $N = 3$.

Choice of N is somewhat arbitrary, and may depend on the known magnitude of the fifth harmonic, for example. Figure 13 compares $f(\xi) = f(x)/\bar{a}^2$ with the approximations (A 2) with $N = 2$ (cubic) and $N = 3$ (quintic) for $-2 \leqslant x/\bar{a} \leqslant 2$, a range very rarely exceeded by a tidal motion. Within this range, both approximations are as close as one can reasonably expect the frictional law to hold physically, bearing in mind that the frictional coefficient k itself varies with velocity.

In the simplified case of a pure sine wave of amplitude $\bar{a}$, (A 2) converges numerically to the Fourier expansion

$$\bar{a}^2 \sin \omega t \, |\sin \omega t| = \frac{8\bar{a}^2}{3\pi} (\sin \omega t - \tfrac{1}{5} \sin 3\omega t - \tfrac{1}{3\,5} \sin 5\omega t - \ldots).$$

One may also use (A 2) to expand harmonically the general case

$$x = \sum_n (a_n \cos \omega_n t + b_n \sin \omega_n t),$$

but this leads to very cumbersome expressions.

PHILOSOPHICAL TRANSACTIONS OF THE ROYAL SOCIETY A MATHEMATICAL, PHYSICAL & ENGINEERING SCIENCES